UNIVERSITY OF CALIFORNIA, SAN DIEGO

Role of Blood-Brain Barrier Leakage during Stroke

A dissertation submitted in partial satisfaction of the

requirements for the degree Doctor of Philosophy

in

Biology with Specialization in Multi-Scale Biology

by

Bo Chen

Committee in charge:

Professor Patrick Lyden, Chair
Professor Colin Jamora, Co-Chair
Professor Jonathan Bui
Professor David Cheresh
Professor Russell Doolittle
Professor Randall Johnson
Professor Maryann Martone

2010

ProQuest LLC
789 East Eisenhower Parkway
P.O. Box 1346
Ann Arbor, MI 48106-1346

The Dissertation of Bo Chen is approved, and it is acceptable in quality and form for publication on microfilm and electronically:

_____

_____

_____

_____

_____

_____

Co-Chair

_____

Chair

University of California, San Diego

2010

DEDICATION

To my family members who have suffered from stroke.

To my parents who have raised me sacrificially.

To my wife, Wenjing, for sharing the faith, hope, and love with me.

TABLE OF CONTENTS

LIST OF FIGURES

Chapter 2

Chapter 3

Chapter 4

Chapter 5

ACKNOWLEDGEMENT

I would like to thank my thesis advisor Dr. Patrick Lyden for his tremendous support during my graduate training. His passion for medicine, his curiosity for better knowledge of the disease, and his dedication in both clinical and translational work have inspired me all the way through. It is a privilege to work with a physician like him, to conceive and design the experiments together. It has been a joyful experience.

I also want to thank my thesis committee members for providing their insights and perspectives that help expand my knowledge in the related field and address a question through multiple approaches. A significant part of the thesis work was inspired by the questions they raised during the committee meetings.

I benefited enormously from the colleagues in the Lyden lab. Dr. Beth Friedman has taught me the first lesson in histology and provided many helpful thoughts and advices. Qun Cheng is a wonderful surgeon and her expertise in animal surgery has ensured the quality and consistency of the experiments. Agnieszka Brzozowska-Prechtl has more than thirty years of experience in histology and her assistance in tissue microtomy has greatly facilitated the progress of my thesis projects. Kai Yang has helped me with fluorescence quantification of the vascular disruption.

I would like to thank colleagues from collaborating labs. Prof. David Kleinfeld has kindly provided the access to fluorescent microscopy in his lab. The

ultrastructural study of the ischemic vasculature was conducted in the National Center for Microscopy and Imaging Research. The experimental design of electron microscopy was supervised by Prof. Maryann Martone, and I also got a lot of technical assistance from Dr. Eric Bushong and Mason Mackey. In my final year of graduate study I worked in Prof. Joan Brown's lab where I started to be involved in the world of cell signaling and biochemistry. The interdisciplinary research environment in UCSD have shaped me and matured my thoughts.

Last but not the least, I want to thank Prof. Terence Hwa who led me into the door of science and serves as a mentor ever since. I thank American Heart Association Predoctoral Fellowship for supporting my research, and Howard Hugh Medical Institute Interfaces Program that provides me the opportunity to use the state-of-the-art imaging methods to explore the biological system at all levels. It has been an amazing journey!

Chapter 2, in full, is a reprint of the material as it appears in Chen B, Friedman B, Cheng Q, Tsai P, Schim E, Kleinfeld D, Lyden PD. Severe blood-brain barrier disruption and surrounding tissue injury. Stroke. 2009 Dec;40(12):e666-74. Permission was obtained from co-authors. I am the primary researcher and author of this paper.

Chapter 3, in part, has been submitted for publication of the material as it may appear in Chen B, Cheng Q, Yang K, Lyden PD. Thrombin mediates severe neurovascular injury during ischemia. Stroke, 2010. Permission was obtained from co-authors. I am the primary researcher and author of this paper.

VITA

Education

2005-2010 Doctor of Philosophy, University of California, San Diego

2001-2005 Bachelor of Science, Peking University, China

Publications

Chen B, Friedman B, Cheng Q, Tsai P, Schim E, Kleinfeld D, Lyden PD. Severe blood-brain barrier disruption and surrounding tissue injury. Stroke. 2009 Dec;40(12):e666-74. *(Cover)*

Chen B, Cheng Q, Yang K, Lyden PD. Thrombin mediates severe neurovascular injury during ischemia. (Accepted)

Chen B, Lyden PD. PAR1 mediates thrombin toxicity affecting vascular disruption and tissue injury during ischemia. (in preparation)

Purcell NP, Chen B, Newton AC, Lyden PD, Brown JH. Effect of PHLPP removal on ischemia/reperfusion injury in the brain. (in preparation)

Honors and Awards

2009 Government Award for Outstanding Students, China Scholarship Council

2009 AHA Predoctoral Fellowship, American Heart Association

2006 HHMI Interfaces Training Grant, University of California, San Diego

2004 Xiyue Scholarship, Peking University

2003 HP Scholarship, China Scholarship Council

2003 President's Undergraduate Research Fellowship, Peking University

2002 Shujuan Scholarship, Peking University

2001 Freshman Scholarship, Peking University

ABSTRACT OF THE DISSERTATION

Role of Blood-Brain Barrier Leakage during Stroke

by

Bo Chen

Doctor of Philosophy in Biology with Specialization in Multi-Scale Biology

University of California, San Diego, 2010

Professor Patrick Lyden, Chair
Professor Colin Jamora, Co-Chair

Stroke is the leading disease accounting for death and disability in the world. It is often caused by the occlusion of blood vessels supplying the brain. Stroke causes the opening of blood-brain barrier (BBB), the specific vascular structure that regulates delivery of substances to the brain. The integrity of the barrier structure depends on a dynamic interaction between endothelial cells, glial cells, and neurons, collectively called the neurovascular unit. BBB breakdown during stroke would allow plasma constituents to enter the brain and possibly damage cells. In this study, I sought to investigate if BBB leakage of plasma toxic factors might contribute to the pathology of ischemic injury.

To address the above question, the first step was to establish the correlation between BBB leakage and tissue injury. Focal ischemia was

produced in a rat model of the middle cerebral artery occlusion (MCAo). High molecular weight dextran-fluorescein isothiocyanate (FITC) was employed to label vascular leakage. A consistent pattern of vascular labeling by dextran-FITC was observed within the ischemic core. Ultrastructural examination showed evidence of cytotoxic edema and severely disrupted vascular membrane associated with the presence of dextran-FITC. Histology revealed that the regional distribution of the severe vascular disruption correlated with the area of the ischemic infarction and neuronal injury. I concluded from these experiments that dextran-FITC can serve as a marker for severe vascular disruption and is useful in further studies of the patho-anatomic mechanisms of vascular-disruption mediated tissue injury.

The next step was to identify the toxic factor that leaks into the parenchymal tissue. Among many candidates, thrombin is one of the earlier mediators responding to endothelial damage. In our stroke model, infusion of thrombin intra-arterially during ischemia greatly exacerbated blood-brain barrier breakdown and severe vascular disruption. Vascular disruption was blocked by intravenous infusion of the direct thrombin inhibitor argatroban. Greater numbers of dying cells were found in regions of severe vascular disruption, and interventions that reduced vascular leakage also reduced the numbers of dying cells, labeled by terminal deoxynucleotidyl transferase dUTP nick end labeling (TUNEL). These experiments suggested a key role for thrombin in mediating cell

demise during ischemia. The next question was to ask how thrombin mediates cell death.

Thrombin may contribute to ischemic injury by potentiating coagulation activity and/or acting on protease-activated receptor 1 (PAR1) on brain cells. To test the specific cellular pathways activated by thrombin, PAR1 antagonist was infused via the jugular vein during ischemia and protected the brain from further vascular damage. Arterial infusion of PAR1 agonist peptide exacerbated the vascular disruption and tissue injury. Immunohistochemistry revealed that PAR1 was activated in regions with vascular leakage. Inhibition of p38 mitogen-activated protein kinase (MAPK), a downstream effector of PAR1, alleviated the ischemic injury. Infusion of an antagonist against platelet aggregation, however, did not affect the ischemic vascular injury and tissue injury. Together, these data suggested a critical role for PAR1/MAPK pathway in thrombin-mediated ischemic injury. Further, the anti-thrombotic function of thrombin antagonists seemed less beneficial, suggesting that thrombin mediated thrombosis during ischemia plays a less significant role than PAR-1 mediated thrombin toxicity.

I. INTRODUCTION

Stroke

Stroke is the leading cause of death and disability in the world. Each year, approximately 795,000 people suffer from stroke in the United States and 15 million worldwide. Clinically, stroke refers to the symptoms produced by the sudden loss of cerebral blood supply. In general, stroke can result from two types of conditions: ischemic stroke occurs when the arteries are occluded by blood clots and hemorrhagic stroke results when the blood vessels rupture and bleed into the brain tissue. Most often, stroke occurs due to the occluded blood vessels and leads to the compromised blood flow to a certain brain territory.

During an ischemic stroke, different brain regions lose cerebral blood flow in a heterogeneous distribution[2-4]. Traditionally, the central area of the stroke is defined as the ischemic core where the blood flow reductions are severe and cells die rapidly. The peripheral area of the stroke is recognized as penumbra where the reduction of blood flow is modest and the cells are able to survive with comprised metabolism. The penumbra region is considered salvageable if reperfused in time, but with extended ischemia duration, the penumbra might evolve into ischemic core and worsen the stroke condition.

Currently there is only one FDA-approved treatment for patients of acute ischemic stroke, through the use of recombinant tissue plasminogen activator (tPA) which initiates blood clot lysis[5]. It improves patient outcomes if applied within three hours of ischemia onset. However, only about 3% of patients nationwide are able to benefit from this treatment due to the three hour temporal

window[6]. With a mortality rate of 30% and disability rate of 30%, stroke remains one of the most challenging medical emergencies for healthcare. The goal of stroke research is to understand the basic mechanisms of the disease and provide new avenues of treatment.

Cell death mechanisms

What causes brain cell injury during ischemia? Ischemic cell death is a complex process engaging interlinked mechanisms and overlapping features[7]. Previous studies have indicated at least three fundamental mechanisms leading to ischemic cell death: excitotoxicity and ionic imbalance, oxidative stress, and apoptotic-like cell death[8].

Excitotoxicity is set in motion soon after the onset of stroke and leads to necrosis in the ischemic core[9-10]. Excitotoxicity starts with the loss of energy stores and the subsequent failure of the ATP-dependent ion channels that result in intracellular ion imbalance and membrane depolarization. As a result, calcium concentration increases and triggers the over-release of glutamate, the major excitatory neurotransmitter in the brain. Extracellular glutamate binds to NMDA and AMPA receptors and promotes the excessive influx of calcium, which induces several lipases and proteases that degrade the membranes and disrupt cellular integrity. Glutamate also binds to ionotropic glutamate receptors promoting excessive influx of sodium that induces cell swelling and edema.

Oxidative stress is mediated by reactive oxygen radicals, most of which are generated by dysfunctional mitochondrial and disrupted electron transport[11-13]. Production of reactive oxygen radicals contribute to ischemia damage profoundly after reperfusion. Those oxygen radicals can directly damage all cellular components such as lipids, proteins, nucleic acids and carbohydrates. In addition, oxygen radicals are related to the activation of the mitochondrial transition pore (MTP), facilitating the release of the pro-apoptosis factors that exacerbate cell death[14-15].

Apoptotic-like mechanisms have been implicated for ischemic cell death, especially in the penumbra area where the ischemic insult is relatively mild. Apoptosis could be triggered by a large number of stimuli including increased calcium signal, free radicals production, DNA damage, and protease activation[16-20]. Both caspase-dependent and caspase-independent mechanisms might be recruited in apoptosis during ischemic stroke[21-22]. More recently, it is suggested that neuronal death occurring in the penumbra region is neither typical necrosis nor apoptosis; instead it appears to be a hybrid that contains pathological features of both[23]. Since apoptosis is an active programmed process that progresses over hours and even days, it is a likely mechanism for delayed ischemic cell death as well.

From the therapeutic point of view, it is important to identify the point at which the cell enters irreversible death process and associate it with certain morphological or biochemical features. In practice, however, this has become

very challenging given the heterogeneous nature of stroke pathology[24-26]. It is not completely understood why a certain group of cells die from a particular injury mechanism. In general, neurons are less resistant to ischemia than astrocytes or endothelial cells[7]. The differential vulnerability also exists among different groups of neurons. Hippocampal CA1 pyramidal neurons suffer from delayed neuronal death after a short global ischemia, whereas CA3 neurons are unaffected[27]. The basis for the heterogeneity of ischemic injury is not clear[9].

Although much progress have been made in understanding the neuronal injury mechanism during ischemic stroke, all the clinical trials targeted to single cellular pathway have failed so far, indicating that a more integrative insight into the cellular and molecular mechanism of ischemic injury is required for the future therapy.

Blood-brain barrier breakdown

Stroke is a vascular disorder affecting neuronal function[28]. Blood-brain barrier serves as an interface between systemic circulation and central nervous system. BBB exists in the capillaries and often refers to the cellular structure composed of endothelial cells, tight junctions, pericytes, basement membrane, and astrocytic end feet[29]. The integrity of BBB is crucial to maintain the homeostasis of the brain. In the condition of ischemic stroke, however, the barrier function can be disrupted resulting in many detrimental effects such as vasogenic edema and hemorrhage transformation[30-31].

BBB damage is often measured by the extravasation of small serum constituents such as albumin and immunoglobulin[32-34]. Extravasation appears in the ischemic territory as early as 30min after the stroke onset, and evolves over hours and even days after reperfusion[35-36]. In addition to the direct endothelial damage, factors that affect BBB permeability include hypoxia, angiogenesis, inflammation, and proteolysis by matrix metalloproteinase (MMP).

The role of hypoxia in BBB damage has been investigated in an *in vitro* model of brain microvessel endothelial cells[37]. Hypoxia induces a rapid increase in intracellular calcium, and triggers several signaling cascades such as calcium/calmodulin-dependent protein kinases (CaMK), extracellular signal-regulated kinase (ERK), and protein kinase C (PKC)[38]. Hypoxia also activates transcription factor hypoxia inducible factor-1 (HIF-1) and promotes production of reactive oxygen species[39-40]. These pathways alter the expression of junctional proteins, such as E-cadherins, claudins, and occludins, and consequently disturb the BBB integrity[37, 41].

The angiogenic response promotes neovascularization and neurogenesis[42-44], and is also accompanied by increased vascular permeability[45-46]. The angiogenic response is initiated by the expression and release of vascular endothelial growth factor (VEGF)[39]. VEGF then binds to VEGF receptor 2 and affects the stability of tight junction complex via the Src kinase pathway[46-47].

Inflammation in the blood-vessel wall and brain parenchymal tissue may both contribute to stroke injury[48-50]. Pro-inflammatory responses are induced within minutes after the brain injury. Increased expression of cell adhesion molecules in endothelial cells mediates the infiltration of neutrophils across the BBB[51]. Other cells including reactive microglia, macrophages, astrocytes and neurons, also generate inflammatory mediators that exacerbate the damage[52].

Matrix metalloproteinase activation has recently been implicated as an important mechanism contributing to BBB injury during stroke[53-54]. Proteolytic activity of MMPs can be triggered by oxidative stress and mitogen-activated protein kinase (MAPK) pathways[55-58]. The gelatinases MMP2 and MMP9 target collagen IV the major component of basement membrane. Other components of tight junction such as occludins might also be degraded by MMPs[59]. Increased levels of MMPs are detected in the blood and brain after ischemia and are associated with increased BBB leakage[60-61].

Central hypothesis

Ischemic stroke involves complex spatial and temporal events evolving over time. The development of ischemic injury is hardly dependent on a single pathway or a single cell type. A growing body of literature has pointed to the importance of the neurovascular unit, a conceptual framework useful to understanding stroke pathophysiology[7, 28]. Neurovascular unit refers to neurons, astrocytes, endothelial cells, and the associated extracellular matrix. An

integrative view of the dynamic interaction within neurovascular unit is crucial to understanding the mechanism of stroke and search for new therapeutic targets.

As reviewed above, blood-brain barrier disruption and parenchymal tissue damage share several injury mechanisms. Reduction of BBB permeability often accompanies decreased infarct volume[62-64]. We therefore asked whether there is a causal relationship between the BBB disruption and tissue injury. The opening of the BBB during stroke not only allows the passage of water into the parenchymal tissue and causes edema, but also provides the possibility for serum constituents to enter the brain and directly induce cellular injury. We hypothesize that blood-brain barrier leakage contributes to ischemic injury by allowing the entry of plasma-derived toxic factors into the brain leading to tissue injury.

To test the hypothesis, first we need to establish the correlation between BBB disruption and tissue injury. Previous attempts to establish a relationship between tissue and vascular injuries have not been successful because of the use of small markers that tend to leak through minimal opening of BBB and spread diffusively beyond the original injury sites. In this study, I proposed to use a large fluorescent marker, 2 MDa dextran conjugated with fluorescein isothiocyanate (FITC), to track vascular disruption, and I developed an imaging analysis method to quantitate the vascular damage. Using this simple imaging technique, I would expect to see larger area of tissue injury with greater vascular damage, and reduced injury as the vascular damage decreased.

The next step was to identify the toxic factor that leaks into the parenchymal tissue. In a catastrophic event like stroke, thousands of molecules in the systemic circulation might invade the brain tissue. A candidate toxic factor should at least possess the following properties: abundant in the blood but not in the normal brain; toxic to neuronal cells; and present in the vascular leakage sites. In this study I focus on thrombin, one of the earliest mediators responding to endothelial damage during ischemia. By promoting or inhibiting thrombin activity during ischemia, I would expect to see increased or decreased level of ischemic injury.

To validate the role of thrombin in causing brain damage after ischemia, it is vital to identify the pathological molecular events that are triggered by thrombin. Thrombin in plasma could exacerbate tissue injury via multiple pathways, of which I study two specific processes: one is to increase coagulant activity and promote thrombosis; the other is to cross the blood-brain barrier and activate the PAR1 receptors on parenchymal tissue cells leading to subsequent cell death. I will interfere with either process to test if one or both contribute significantly to tissue damage induced by thrombin. The results of the experiments will provide insights to the critical molecular events in focal ischemia, and will indicate important target molecules for treatment of stroke.

II. SEVERE BLOOD-BRAIN BARRIER DISRUPTION AND SURROUNDING TISSUE INJURY

Severe Blood–Brain Barrier Disruption and Surrounding Tissue Injury

Bo Chen, BS; Beth Friedman, PhD; Qun Cheng, MD; Phil Tsai, PhD; Erica Schim, MD; David Kleinfeld, PhD; Patrick D. Lyden, MD

Background and Purpose—Blood–brain barrier opening during ischemia follows a biphasic time course, may be partially reversible, and allows plasma constituents to enter brain and possibly damage cells. In contrast, severe vascular disruption after ischemia is unlikely to be reversible and allows even further extravasation of potentially harmful plasma constituents. We sought to use simple fluorescent tracers to allow wide-scale visualization of severely damaged vessels and determine whether such vascular disruption colocalized with regions of severe parenchymal injury.

Methods—Severe vascular disruption and ischemic injury was produced in adult Sprague Dawley rats by transient occlusion of the middle cerebral artery for 1, 2, 4, or 8 hours, followed by 30 minutes of reperfusion. Fluorescein isothiocyanate-dextran (2 MDa) was injected intravenously before occlusion. After perfusion-fixation, brain sections were processed for ultrastructure or fluorescence imaging. We identified early evidence of tissue damage with Fluoro-Jade staining of dying cells.

Results—With increasing ischemia duration, greater quantities of high molecular weight dextran-fluorescein isothiocyanate invaded and marked ischemic regions in a characteristic pattern, appearing first in the medial striatum, spreading to the lateral striatum, and finally involving cortex; maximal injury was seen in the mid-parietal areas, consistent with the known ischemic zone in this model. The regional distribution of the severe vascular disruption correlated with the distribution of 24-hour 2,3,5-triphenyltetrazolium chloride pallor ($r=0.75$; $P<0.05$) and the cell death marker Fluoro-Jade ($r=0.86$; $P<0.05$). Ultrastructural examination showed significantly increased areas of swollen astrocytic foot process and swollen mitochondria in regions of high compared to low leakage, and compared to contralateral homologous regions (ANOVA $P<0.01$). Dextran extravasation into the basement membrane and surrounding tissue increased significantly from 2 to 8 hours of occlusion duration (Independent samples t test, $P<0.05$).

Conclusion—Severe vascular disruption, as labeled with high-molecular-weight dextran-fluorescein isothiocyanate leakage, is associated with severe tissue injury. This marker of severe vascular disruption may be useful in further studies of the pathoanatomic mechanisms of vascular disruption-mediated tissue injury. **(*Stroke*. 2009;40:e666-e674.)**

Key Words: blood–brain barrier breakdown ■ endothelial cells ■ stroke

Pathological responses to ischemia in the microvasculature play a central role in the evolution of infarction; a critical event after ischemia is blood–brain barrier (BBB) breakdown,[1] an antecedent event to cerebral infarction and hemorrhagic transformation.[2] Increasing awareness of the interplay between vessels, glia, and neurons has led to improved understanding of the mechanisms of infarction[3] and has partially begun to explain the failures of previous neuroprotective therapies. In parallel with new understanding of the neurovascular and glial-vascular unit, preliminary data suggest direct cytotoxicity of serum constituents, such as thrombin and plasminogen,[4] in addition to the toxic effects of water entry caused by oncotic pressure shifts. The sequence of events is complex, however, because these same compounds also could occur de novo in injured parenchyma, or in the endothelium. Traditional studies of BBB leakage relied on simple measures of water flux (edema), leakage of small-molecular-weight markers (IgG or albumin labeled with Evan Blue), or very complicated and expensive ultrastructural imaging of endothelial cells, so it has been difficult to fully characterize the pathoanatomic mechanisms of injury after severe vascular disruption and to separate the effects of edema (water shift) from other putative toxic molecules. Further progress in these investigations is limited by: (1) a paucity of data regarding the time course of BBB leakage to differentially sized markers; (2) the absence of a simple, reliable marker of severe vascular disruption; and (3) quantitative measurements of leakage over time after severe

Received February 27, 2009; final revision received June 25, 2009; accepted July 24, 2009.

From Department of Neurosciences (B.C., B.F., Q.C., E.S., P.D.L.), University of California San Diego, School of Medicine, La Jolla Calif; Veterans Administration Medical Center (B.F., Q.C., P.D.L.), San Diego Calif; Department of Physics (P.T., D.K.), University of California San Diego, La Jolla Calif.

B. Chen and B. Friedman contributed equally to this work.

Correspondence to Dr Patrick Lyden, 3350 La Jolla Village Drive, San Diego, CA 92161. E-mail lydenp@cshs.org.

Stroke **is available at http://stroke.ahajournals.org** **DOI: 10.1161/STROKEAHA.109.551341**

vascular disruption. We sought to characterize severe vascular disruption with high-molecular-weight dextran-fluorescein isothiocyanate (FITC) using fluorescent, immunohistochemical, and ultrastructural confirmation, and then compared such vascular disruption to evidence of tissue injury.

Materials and Methods

All protocols were approved by the Animal Research Committee of the Veteran's Affairs Medical Center, San Diego, and by the IACUC of University of California San Diego, following all national guidelines for the care of experimental animals. The (n=71) subjects were adult male Sprague-Dawley rats (Harlan, San Diego, Calif), and average weight was 300 grams. All animals received tail-vein injections of FITC conjugated to a high-molecular-weight dextran (2 MDa; Sigma); 0.3 mL of 5% (wt/vol) solution in sterile phosphate buffered saline (PBS) at the start of surgery, eg, ≈20 minutes before occlusion of the middle cerebral artery. The subjects were allowed to awaken from anesthesia during the occlusion and reperfusion periods to allow neurological examinations with a dichotomized version of the published rodent neurological grading system.[5,6] To assure sufficient ischemia with the middle cerebral artery occlusion, only animals that registered abnormal on 3 behavioral signs were used; otherwise, the subject was excluded from further analysis. Animals were also excluded for subarachnoid hemorrhage found at postmortem dissection.

We used our version of the standard model of filament occlusion of the middle cerebral artery.[5,7] Briefly, animals were induced with isoflurane anesthesia and maintained with a mixture of 4% isoflurane in oxygen:nitrous oxide 30:70 by face mask. After adequate anesthesia and aseptic preparation, an incision was made in the neck, exposing the left common carotid artery. The external carotid and pterygopalatine arteries were ligated with 4-silk. An incision was made in the wall of the common carotid artery, which was then threaded with a 4-0 nylon suture (Ethicon) that was blunted in a microforge (Narishige MF83); filament diameters were measured using microscopy and image analysis and only filaments between 290 and 310 μm were selected for further use. The suture was advanced 17.5 mm from the bifurcation point of the external and internal carotid arteries, thereby blocking the ostium of the middle cerebral artery. At the end of the reperfusion period, the rat was euthanized with an overdose of pentobarbital and then intracardially perfused with 200 to 300 mL saline followed by 300 mL of 4% (wt/vol) paraformaldehyde in PBS.

After rapid removal from the skull, each brain was postfixed in 4% (wt/vol) paraformaldehyde in PBS and then cryoprotected in 30% sucrose to obtain 50-μm-thick sections with a freezing sliding microtome. To characterize the distribution of high-molecular-weight dextran–FITC, sequential sections through the anterior–posterior axis of the middle cerebral artery territory subsuming ≈4.5 mm of brain were sampled from ≈−0.3 bregma as an anchoring level and mounted onto glass slides. Sections were cover-slipped with Prolong Gold Antifade mountant (Molecular Probes). An additional series of sections was slide-mounted for determination of regional colocalization in the ischemic striatum of retained fluorescein with neuronal degeneration marked by Fluoro-Jade C-staining (Chemicon). Sections processed for immunocytochemistry for light microscopy incubated free-floating in antibody solutions and endogenous peroxidase was quenched with a 10-minute incubation in 3% (v/v) hydrogen peroxide in PBS. Primary antibody (anti-universal IgG; Vector) was diluted in a blocking diluent (PBS with 10% [v/v] blocking serum and 0.2% [v/v]; Triton X-100) was applied for 2 days and was followed by incubation for 4 hours in biotinylated antirabbit secondary antibody diluted in blocking diluent. Biotinylated secondary antibody was visualized by overnight incubation of sections in Cy5-conjugated streptavidin (Jackson Immunoresearch). Fluorescent immunostained sections were mounted on slides and cover-slipped with Pro-Long Antifade mountant (Molecular Probes). Background staining was assessed in sections processed without primary antibody. For ultrastructural localization of high-molecular-weight dextran–FITC after stroke, animals were prepared for transcardial perfusion–fixation and perfused with Ringer solution, followed by 4% paraformaldehyde and 0.1% glutaraldehyde in PBS solution. Brains were removed from the skull, fixed in 4% buffered paraformaldehyde overnight, and cut into 100-um thick slices on a Leica VT1000S microtome. Bound fluorescein was visualized by incubation of sections with biotinylated antifluorescein antibody (BA-0601; Vector; 1:1000 dilution) for 1 day followed by peroxidase catalysis of diaminobenzidine reporter (ABC kit PK6100 Vector and diaminobenzidine kit, SK4100; Vector). Immunostained brain slices were postfixed in 2.5% glutaraldehyde for 15 minutes on ice and then 1% osmium tetroxide for 1 hour, dehydrated, embedded in Durcupan, sectioned at 50 nM on a Reichert-Jung Ultracut E system, and mounted on coated copper grids.

Fluorescence from retained high-molecular-weight dextran–FITC was quantified within the hemisphere by semiautomated image analysis. Digitized images of the ischemic half of the brain were taken with a Zeiss microscope outfitted with CCD camera (KAF32MB; Apogee). Images were obtained at 500-μm intervals across the anterior-to-posterior axis of the middle cerebral artery territory. Fluorescence was quantified using Image Pro Plus (Cybermedia). An operator without knowledge of the subject's group or occlusion duration examined each section after first setting the magnification and performing a linear calibration using a scale bar. The operator then examined each section and set the brightness and contrast levels to optimize the appearance of the fluorescence. Using semiautomated thresholding, segmentation, and size filtering, the operator measured the total area of fluorescence. Total fluorescence typically consisted of multiple discrete "islands" on each section, and within each island there were pale areas of extravasated label intermixed with areas of very bright vascular labeling. Using an image of the islands as an overlay, the operator then re-thresholded to emphasize the bright objects contained within the islands of total fluorescence, ie, labeled vessels, and, again using segmentation and size filtering, the area of all bright vessels was measured. The area of extravasation was obtained by subtracting the area of bright fluorescence in the vessels from the total area fluorescence.

To quantify the presence of multiple fluorescent markers on single sections, we adapted a laser-scanning technique. Image acquisition was performed on an Olympus BX50 Microscope retrofitted with a CompuCyte laser scanning cytometry acquisition system. Tissue was illuminated with a focused argon laser (488 nm), and fluorescein fluorescence was collected through an emission filter of 530±30 nm. Cy5 fluorescence was illuminated with a focused helium–neon laser (633 nm), and fluorescence was collected through an emission filter bandwidth of 675±50 nm. The fluorescence was averaged over 20-μm-diameter bins (scanned areas) that encompassed the entire tissue section. Histograms were constructed to plot the regions of interest or "counts" as a function of integrated fluorescence intensity in those areas.

Background was determined by scanning subareas on the nonoccluded side of the section to obtain a histogram of the distribution of background signals. We conservatively determined a threshold for "signal" according to the maximum level of tissue background. Data were expressed as the number of scanned areas detected above background fluorescence intensities, divided by the total number of scanned areas/section. In cases with fluorescent immunostaining, similar routines were imposed to quantify immunostained regions of interest in register with fluorescein–dextran retention sites. The percent of counts with double fluorescent signals (fluorescein and Cy5) was determined from scattergram plots that were divided into 4 quadrants using Wincyte software (CompuCyte Corp).

Two-photon laser scanning microscopy was used to scan and reconstruct labeled vessels and extravasated fluorescent markers. Stacks of optically sectioned images were acquired with a 2-photon laser scanning microscope of custom design[8] using the MPScope software.[9] We used a 40×, 0.8-NA water dipping objective (IR Achroplan; Carl Zeiss Inc), 0.4 μm per pixel lateral sampling, and 0.5 μm per plane axial sampling. FITC–dextran was excited at 800

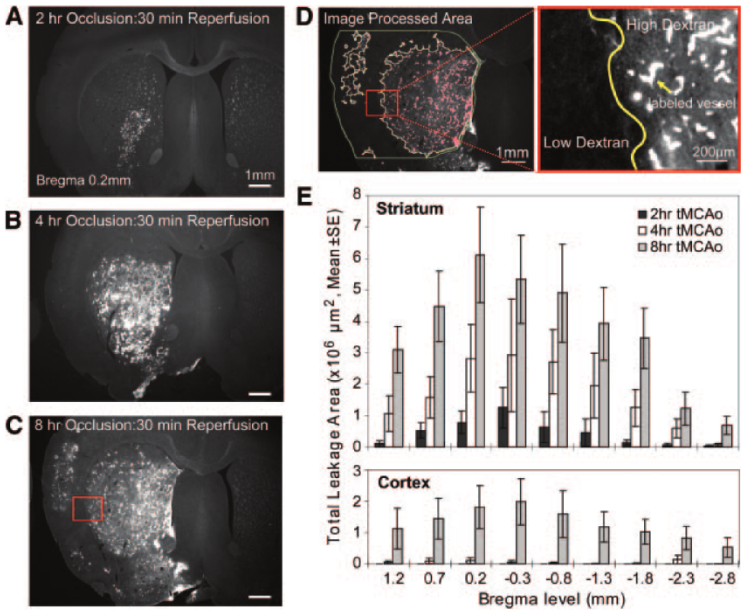

Figure 1. Severe vascular disruption after ischemic injury. Transient middle cerebral artery occlusion using a nylon filament at 2 hours (n=9), 4 hours (n=9), or 8 hours (n=6), was followed by 30 minutes of recirculation after filament removal. High-molecular-weight dextran–FITC fluorescence was measured by thresholding and semiautomated quantitation of 50-μm coronal sections obtained in the mid-parietal cortex. A, Two-hour transient middle cerebral artery occlusion and 30 minutes of reperfusion caused accumulation of the high-molecular-weight dextran in medial striatum, ipsilateral to the middle cerebral artery occlusion. B, Occlusion for 4 hours caused greater retention of the label, subsuming lateral striatum. C, The 8-hour occlusion resulted in involvement of the entire striatum and isolated areas in the cortex. The section shown in (C) is shown again in (D) after semiautomated processing, including thresholding, segmentation, and object delineation in the areas of fluorescence that could be quantified. Next to the processed view in (D), a higher magnification view of the area marked by the red box demonstrates fluorescence retention in the vessels and extravasation into parenchyma. E, Consecutive coronal levels separated by 500 μm were selected from anterior to posterior and quantified. With increasing duration of ischemia, there was a progressive accumulation of high-molecular-weight dextran–FITC in the striatum and cortex supplied by the middle cerebral artery (overall 1-way ANOVA for time, $P<0.0001$). Note the delay in accumulation in the cortex relative to striatum.

nm and the fluorescence was detected by low-pass filtering of the emission light <700 nm. Image rotation and projection operations were performed with the ImageJ software program. (NIH).

Blocks for plastic embedding were selected, based on the immunostaining for high-molecular-weight dextran–FITC, and categorized as originating from a region of high or low leakage. Blocks were also selected from homologous regions in the contralateral hemisphere. After processing as described, images were taken at 5000× on a JEOL 1200EX microscope. An examiner blind to the region of origin for each image then placed a 6×6 grid (with an interval of 2 μm between grids) on the images centered on a vessel. Using standard stereological technique,[10] the grid crossings that hit the swollen astrocytic food processes or structureless space were counted as points of "swollen cells." For the points aligning on the boundary of grids, only those on the right and bottom were counted. To normalize the results, the points that corresponded to an area of endothelial cells (including lumen space) were counted as well. Enlarged abnormal mitochondria were counted separately in each field of view. The point counts were summarized and normalized to the containing space, standardized to the calibrated grid.

Results

Vascular Disruption After Transient Middle Cerebral Artery Occlusion

Transient middle cerebral artery occlusion caused uptake of circulating high-molecular-weight dextran–FITC into vessels and extravasation into parenchyma as shown in Figure 1. The rest of the tissue section was not fluorescent because the saline perfusion removed intravascular dextran–FITC at euthanization.[11] At longer occlusion times, the subregional distribution of fluorescence expanded to include the more lateral aspect of the striatum (Figure 1B). Islands of leakage appeared in the cortex after 8 hours of middle cerebral artery occlusion (Figure 1C). Image analysis identified regions showing both labeling of the vessel walls as well as parenchymal extravasation (Figure 1D). With increasing occlusion duration, vascular damage increased in the regions supplied by the middle cerebral artery, as indicated by a significant increase in the accumulated dextran–FITC (Figure 1E).

Localization of Vascular Pathology to Regions of Severe Vascular Disruption

To demonstrate that the extravasated fluorescence seen in Figure 1 was truly extravascular, we used 2-photon imaging to optically section and reconstruct a labeled vessel and adjacent leakage (Figure 2). Epifluorescence microscopy demonstrates a swath of intensely fluorescent vessel segments (Figure 2A) on the ischemic side of the brain. In a subset of labeled vessels, a hazy fluorescence also appeared to extend into the neighboring parenchyma (Figure 2B). In the 2-photon maximal projections (Figure 2C, 2D), the intense vascular fluorescence was associated with the vessel

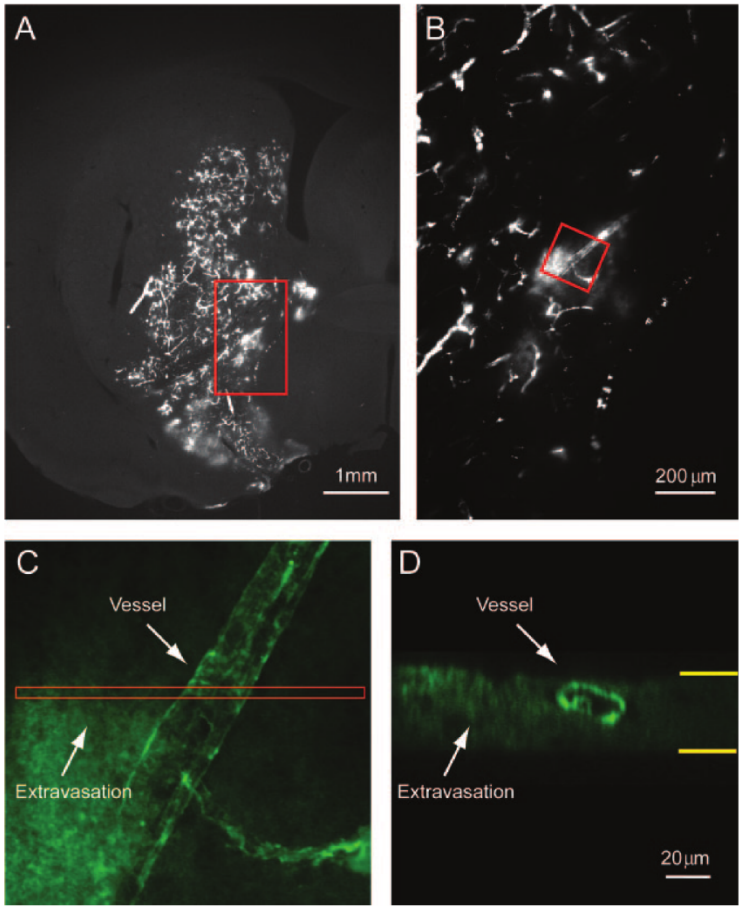

Figure 2. High-molecular-weight dextran–FITC localizes to the vessel wall and extravasates. Extravasation of high-molecular-weight dextran–FITC was measured in the regions of brain subjected to severe ischemia. A, Epi-fluorescent image of a section from a rat with 4-hour middle cerebral artery occlusion shows vascular labeling and extravasation as in Figure 1. B, Photomicrograph of vessels identified with FITC–dextran and extravasation in the surrounding tissue. C, Image of the region outlined in (B) obtained using 2-photon laser scanning microscopy. An image stack was taken across the entire tissue section and axially projected as an average across all frames. Uptake of high-molecular-weight dextran–FITC is evident in both the large vessel as well as the smaller branch at the lower right of the image. Leakage of the dextran–FITC into the parenchyma can be seen in lower left quadrant of the image. D, A side projection of the highlighted region of the 2-photon laser scanning microscopy image stack shown in (C). The vessel cross-section shows a hollow vessel lumen. The projection is an average across 4 μm and spans the entire axial extent of the tissue section, ensuring that the fluorescence seen to the left of the vessel is caused by leakage, presumably from the imaged vessel.

wall. The vessel lumen was clear (Figure 2D), consistent with the effective washout of labeled plasma with transcardial perfusion fixation. This suggests that macromolecular dextran–FITC can lodge at high concentrations in ischemic endothelial cells and also escape from these vessels into surrounding parenchyma. Animals (n=6) were infused with high-molecular-weight dextran–FITC intravenously and then subjected to transient middle cerebral artery occlusion of 2 or 8 hours, followed by 30 minutes of reperfusion. Sections from the mid-parietal cortex were processed for optimal ultrastructural visualization as noted, and 3 blocks of tissue were selected based on the pattern of high-molecular-weight dextran–FITC labeling to include regions with high dextran distribution, low dextran distribution, and contralateral site (Figure 3). To image the ultrastructural deposition of bound fluorescein–dextran, the tissue was reacted with antifluorescein antibody and converted to diaminobenzidine, an electron-dense reaction product. Ischemic vessels that were labeled with diaminobenzidine were distinguished by electron-dense cytoplasmic labeling in constituent endothelial cells. These labeled endothelial cells were typically swollen (Figure 3C). Endothelial cells of vessels from low leakage ischemic areas or from the contralateral side were not obviously enlarged (Figure 3D, 3E). We used stereological analysis to quantify ultrastructural changes in tissues surrounding vascular disruption as labeled with high-molecular-weight dextran–FITC (Figure 4). Ipsilateral to the occlusion, the total areas of endothelial cells (including lumena) were slightly decreased compared to the opposite control side, consistent with edematous compression (data not shown), but the ratio of endothelial cell area to lumen was markedly increased in areas of high leakage, compared to areas of low leakage or contralateral side (Figure 4C; $P<0.001$; 1-way ANOVA; Tukey post hoc test). We demonstrated significant increases in the density of swollen mitochondria and astrocytes, and empty voids indicative of severe edema (Figure 4C). In regions of high leakage, the average area of astrocytic end-feet and structureless spaces were significantly larger—consistent with swelling as seen in cytotoxic edema—compared to areas with lower amounts of high-molecular-weight dextran–FITC signal, or corresponding subregions on the contralateral side ($P<0.001$; 1-way ANOVA; Tukey post hoc test). Greater numbers of swollen mitochondria were found in association with vascular labeling with high molecular weight dextran–FITC (Figure 4C; $P<0.001$; 1-way ANOVA; Tukey post hoc test).

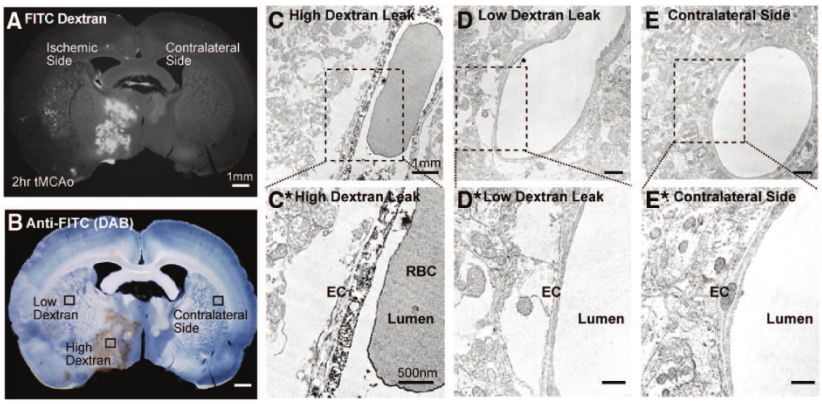

Figure 3. Ultrastructural localization of high-molecular-weight dextran–FITC. The localization of fluorescence (A) was confirmed using anti-FITC and a secondary reporter imaged with diaminobenzidine (B). Using FITC fluorescence on vibratome sections, we selected blocks from regions of high dextran accumulation, low dextran accumulation, and homologous sections from the contralateral sides. Ultrastructural examination at 5000× magnification revealed significant vascular labeling of the endothelial cells in regions of high-dextran fluorescence (C) and far less labeling in regions of low-dextran fluorescence (D) or the contralateral side (E). Higher-power views of the selected regions of interest are shown in C*, D*, and E*, respectively. C* demonstrates label contained in endothelial cells and some gross poration of the cell membrane.

Localization of Tissue Damage to Regions With Severe Vascular Disruption

We demonstrated tissue damage associated with areas of severe vascular disruption using multiple approaches. In 11 animals with variable durations of occlusion followed by reperfusion until 24 hours after onset of occlusion, the area of high-molecular-weight dextran–FITC leakage correlated well with the volume of tissue damage as labeled by 2,3,5-triphenyltetrazolium chloride staining (Figure 5; correlation coefficient $r=0.75$; $r^2=0.56$; $P<0.05$). Neuronal degeneration, labeled with Fluoro-Jade, was also observed in regions of high-molecular-weight dextran–FITC leakage in 10 animals (Figure 6; $r=0.86$; $r^2=0.75$; $P<0.05$). These findings together establish that high-molecular-weight dextran–FITC leakage serves to identify areas of severe vascular disruption and ischemic tissue injury.

BBB Leakage Areas Exceed Areas of Severe Vascular Disruption

To determine whether vascular disruption labeled with high-molecular-weight dextran–FITC merely served to identify areas of BBB leakage, which could be reversible, we compared the distribution of IgG leakage to vascular disruption in 20 animals (Figure 7). We found a significant dissociation between BBB leakage as labeled with IgG, compared to areas of severe vascular disruption, at multiple durations of middle cerebral artery occlusion (Figure 7; 1-way ANOVA; $P<0.001$; Tukey post hoc test). At all occlusion durations, the area of BBB leakage greatly exceeded the area of vascular disruption. The extent of BBB leakage reached a maximum by 4 hours of occlusion; but in contrast, the time course of severe vascular disruption was slower and showed greatest leakage at 8 hours, the longest duration we studied.

Discussion

Our data demonstrate that severe vascular disruption allows passage of high-molecular-weight dextran–FITC that is time-dependent and maximal in the brain regions made ischemic after occlusion of the middle cerebral artery (Figures 1, 2, 3).[12] With longer durations of ischemia, the high-molecular-weight dextran–FITC label accumulates with greater concentration in areas of basal lamina disruption, endothelial and astrocytic swelling, and eventually with total vascular poration (Figures 3, 4). Further, as the degree of vascular disruption increases, there is a corresponding increase in the extent of associated tissue damage (Figures 4, 5, 6). The label can be used to identify regions of brain undergoing severe vascular disruption as early as 1 hour after onset of ischemia (Figure 7). This suggests that brain regions suffering the most severe degree of ischemic injury after vascular occlusion can be labeled easily with a simple intravenous infusion of an inexpensive fluorescent maker. As shown in Figure 3, the presence of the marker can be used to select tissue that is undergoing significant vascular disruption and tissue damage for further detailed study. To our knowledge, this is the first simple marker of severe tissue injury that can be used easily and reproducibly as early as 1 hour after ischemia onset. We used high-molecular-weight dextran–FITC leakage to demonstrate a significant downregulation of the Aquaporin 4 receptor in regions of severe vascular disruption, further supporting the relationship between severe vascular disruption and tissue injury.[13]

The loss of BBB function in ischemic vasculature has been extensively studied and well-established with a variety of quantifiable tracers including isotopically labeled proteins and amino acids,[14–18] isotopically labeled sucrose,[19] fluorescent tracers,[20–22] and with MRI contrast agents.[23] Typically, quantification is made in terms of average vessel leakiness. The time course of increased leakage observed in the present study is consistent with that observed by previous spectrophotometric methods.[21] Additionally, the gross regional specificity of our results are consistent with the low-resolution spatial patterns of BBB observed with MRI, which demon-

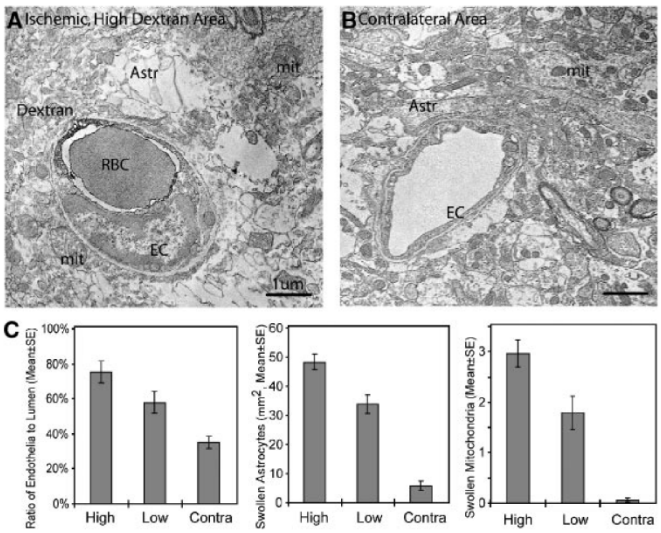

Figure 4. Vascular disruption and cytotoxic edema results in areas of high-molecular-weight dextran leakage. Using tissue blocks from areas of high- or low-dextran accumulation and the homologous contralateral sections (n=6) selected as in Figure 2, we examined serial 50-nm-thick sections. Using an unbiased stereological counting grid, we estimated the areas of endothelial cells and astrocytes, as well as the areas of "featureless void" that likely represent water accumulation. We also identified swollen mitochondria by visual inspection, defined as mitochondria appearing to be twice the size or larger of mitochondria seen on the contralateral region. Note that in areas of significant accumulation of fluorescent high-molecular-weight dextran (A) there are extremely swollen astrocytes (Astr) and mitochondria (mit). Also, the cytoplasm of the endothelial cells is greatly expanded, compared to the contralateral side (B) or the low-dextran region (not illustrated). The averaged results from 138 sections are summarized with standard errors in (C). Because of the opposite effects of cytoplasmic swelling and luminal compression caused by edema, the total endothelial areas (including lumen) are approximately comparable between areas of high and low dextran accumulation, and both are somewhat less than the contralateral side (data not shown). The ratio of endothelial cell area to lumen area (C, left panel) clearly demonstrates significant cytotoxic edema and luminal compression in areas of high leakage, compared to areas of lower leakage and the contralateral side (ANOVA $P<0.001$; Tukey test for posthoc comparisons). The accumulation of increasing quantities of high-molecular-weight dextran–FITC was significantly associated with astrocyte swelling (C, middle panel; ANOVA $P<0.0001$; using Tukey test for post hoc comparisons; all pair-wise comparisons were significant; $P<0.01$). Similarly, the number of swollen mitochondria per field increased with increasing dextran accumulation (C, right panel; ANOVA $P<0.0001$; using Tukey test for post hoc comparisons; all pair-wise comparisons were significant; $P<0.01$).

strate early contrast enhancement (2.5 hours of occlusion) in the ventral striatum of the adult rat.[23]

The mechanism of high-molecular-weight dextran leakage is not established unequivocally by our data, although inspection of the ultrastructure (Figures 3, 4) suggest that both increased transcytosis and gross cellular poration are involved. Using similar approaches, the leakage of small-molecular-weight albumin was shown to precede and show more extensive staining than the leakage of large-molecular-weight dextran.[12] Considerable literature addresses the leakage of smaller-molecular-weight molecules via loosening of the tight junctions between endothelial cells, but there is debate over the roles of transcytosis and transmembrane poration.[24–26] Our data do not address the role of tight junction loosening in the mechanism of higher-molecular-weight dextran leakage, but the time course and spatial distribution of vessel ischemia, as demonstrated by high-molecular-weight dextran–FITC uptake, is consonant with the molecular events that underlie BBB breakdown after experimental large vessel occlusion.[27] Proteolytic breakdown of BBB structural molecules[19] is an early event that occurs within 1 to 2 hours after an ischemic insult.[19,27–31] Immunocytochemical imaging studies of molecular changes in other neural compartments illustrate that they also occur in a spatially heterogeneous fashion,[32,33] forming "islands" of altered protein expression that have been purported to represent small infarctions in both the ischemic striatum and cortex. The temporal and spatial development of severe vascular disruption (Figure 1) appears to coincide with these well-documented molecular events and whereas our data do not allow us to confirm a mechanistic link, the technique we present here will greatly facilitate such mechanistic investigations in the future.

Our study comes with some limitations. High-molecular-weight dextran–FITC is detected directly, without amplification; other markers, including the low-molecular-weight marker IgG, are detected after antibody labeling, which could amplify the signal. The degree of difference between IgG leakage vs high-molecular-weight dextran leakage (Figure 7) likely exceeds the possible amplification step, but such an effect cannot be excluded by our data. Tissue injury markers such as 2,3,5-triphenyltetrazolium chloride exclusion and Fluoro-Jade uptake, although standard in the field, are not synonymous with cell death, nor do they differentiate between necrotic and apoptotic cell death mechanisms. We cannot assert that the severe vascular disruption identified with high-molecular-weight dextran–FITC marks regions of brain undergoing

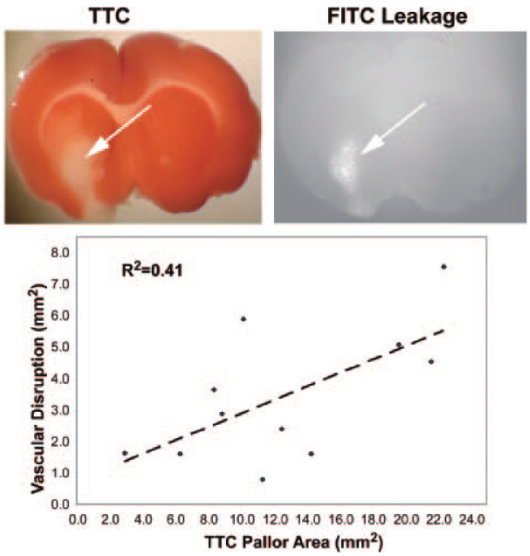

Figure 5. Accumulation of high-molecular-weight dextran–FITC in areas of significant tissue injury. Vascular disruption was compared to tissue injury after varying durations of ischemia (2 hours, n=4; 3 hours, n=5; 4 hours, n=1; each time point marked with a different symbol). High-molecular-weight dextran–FITC was administered before middle cerebral artery occlusion, and again just before euthanization. After 24 hours of reperfusion and euthanization, brains were immediately processed in 2,3,5-triphenyltetrazolium chloride to visualize the region of cellular injury and photographed. The sections were then fixed, imaged, and photographed under fluorescence optics. Scrambled identifiers were used to label the 2,3,5-triphenyltetrazolium chloride and the fluorescent images. Using calibrated planimetry, one examiner traced the areas of 2,3,5-triphenyltetrazolium chloride pallor and then traced the area of fluorescence in a masked fashion. After unblinding, the measurements were linked and compared. The scatterplot shows 10 data pairs. There was a significant correlation between 2,3,5-triphenyltetrazolium chloride pallor and the accumulation of high-molecular-weight dextran–FTIC (Pearson r=0.75; P=0.05; R^2=0.56).

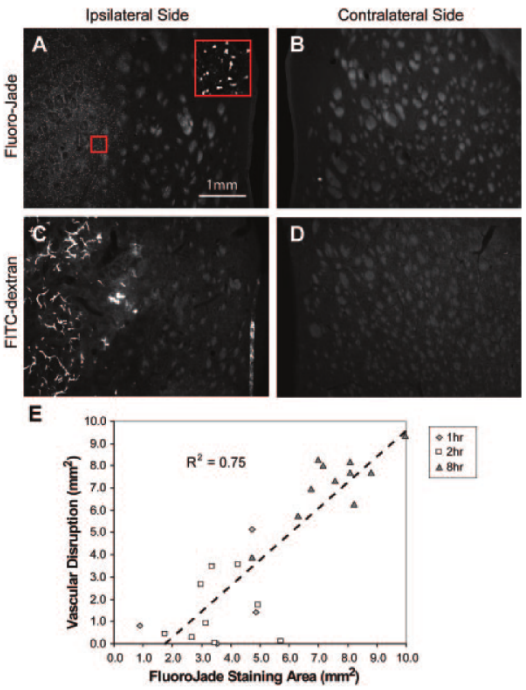

Figure 6. Significant cytopathology results in areas of accumulation of high-molecular-weight dextran–FITC. In the hemisphere ipsilateral (A) and contralateral (B) to the middle cerebral artery occlusion, we compared the extent of cytotoxic injury (using the cell-injury marker Fluoro-Jade) to the area of accumulation of high-molecular-weight dextran–FITC in the ipsilateral (C) and contralateral (D) hemispheres. On high-power examination (inset in A), the Fluoro- Jade is clearly localized to cell bodies that resemble neurons, but cell-specific markers were not used to differentiate neurons from astrocytes. As in Figure 5, a single examiner traced the areas of Fluoro-Jade uptake and, in a masked fashion, independently traced the areas of dextran accumulation (n=10 animals, 2 to 3 sections per animal, ischemia durations of 1 hour, n=3; 2 hours, n=3; 8 hours, n=4; each time point marked with a different symbol). After unblinding and linking the measurements, there was a highly significant relationship between the leakage marker and cytopathology (Pearson r=0.86; P<0.05; R^2=0.75).

irreversible ischemic damage that will inevitably become infarct, although it is difficult to believe that areas showing such severe injury (Figures 3, 4) could recover. Further studies are needed to: (1) show that such marked areas do not possess the ability to recover; (2) identify the mechanisms of severe vascular disruption; and (3) determine if protective agents that inhibit severe vascular disruption also block the associated tissue injury. Another limitation is the relatively biased sampling strategy we used for selecting sections for ultrastructure. A purely random sampling strategy would be unbiased, and might allow one to determine whether evidence of severe vascular disruption is found only in areas of greatest high-molecular-weight dextran leakage. However, such a sampling strategy is difficult for cost and time reasons. To overcome this selection bias, all sections were reviewed in semi-blinded fashion. In other words, in double-labeling experiments, images were taken from all sections using one label, then scrambled, and all sections were reimaged using the second label. Similarly, in the planimetry and point-counting assessments, the investigator examined all sections of one label, and then reviewed all the sections using the other label after scrambling de-identified sections. With these limitations in mind, the argument that high-molecular-weight dextran leakage occurs in areas of vascular disruption and tissue injury is supported by the fact that we used multiple, complimentary imaging techniques, all of which clearly show the same, highly statistically significant relationship. We specifically hypothesized that vascular disruption and tissue injury would occur in areas of greater dextran leakage, and our data support this hypothesis directly (Figures 5, 6).

We have demonstrated that a simple, inexpensive, intravenous marker—high-molecular-weight dextran–FITC—reproducibly labels brain regions undergoing severe vascular disruption and associated tissue injury before the development of obvious infarction. Labeling is greatest in the regions

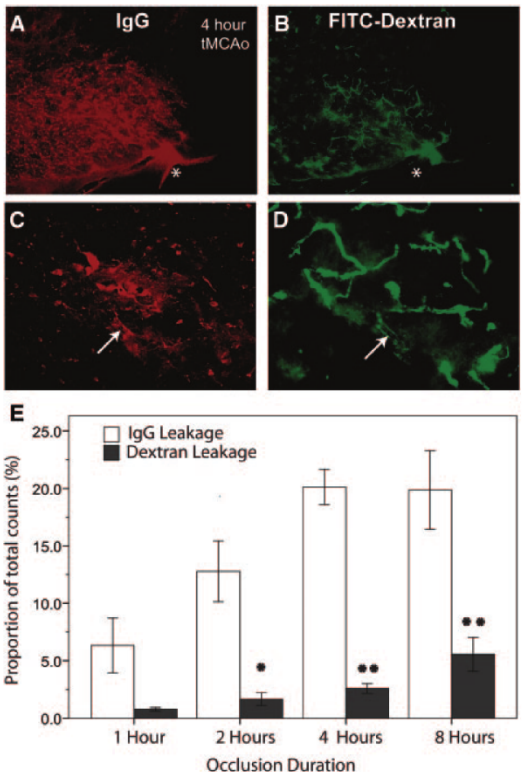

Figure 7. Vascular disruption occurs within a larger region of BBB leakage. After 1 hour (n=4), 2 hours (n=5), 4 hours (n=5), or 8 hours (n=6), middle cerebral artery occlusion followed by 30 minutes of reperfusion, we measured the quantities of IgG and high-molecular-weight dextran in the images, using double-labeled fluorescence microscopy. Fluorescence was quantified with laser scanning microscopy, and the counts in each channel normalized to the total counts present in the section. A, In a representative example, IgG leakage (Cy5 channel) appeared to be more homogenous and not confined to vessels. B, The same section was imaged using the FITC channel, showing a much more heterogeneous appearance and localization to the vessels. The asterisk (*) is placed in the ventricle to demonstrate image registration. Higher-magnification views of IgG leakage (C) and high-molecular-weight dextran leakage (D) confirm the vascular localization of the dextran; the arrows point to a vessel with significant retention of IgG and, in a more heterogeneous pattern, dextran–FITC. The average proportions with standard errors are shown for each occlusion duration (E). The proportion of counts showing the IgG leakage (Cy5) exceeded the proportion showing dextran leakage (FITC) in all sections studied at all time points (independent samples *t* tests, $P<0.05$ after Bonferroni correction). Leakage of IgG appeared to reach a maximum by 4 hours of middle cerebral artery occlusion, but dextran leakage appeared to increase at each time point up to 8 hours (1- way ANOVA for time, $P<0.001$ for dextran).

of brain known to suffer the greatest degree of ischemia after middle cerebral artery occlusion and increasing durations of ischemia cause greater amounts of labeling. This marker will allow for further studies of the mechanisms of vascular injury, and the relationships between vascular, glial, and neuronal cell injury mechanisms, by providing a simple way to identify severely damaged tissue as early as 1 hour after ischemia onset.

Acknowledgments

The authors thank Rodolfo Figueroa for fabricating occluding filaments, Kai Yang for assisting in fluorescence quantification, Judy Norberg for performing the laser scanning cytometry, Dr Maryann Martone for helpful suggestions in ultrastructural imaging, and Drs Donald Pizzo and the late Leon Thal for use of their photomicroscope. B.C. thanks the HHMI-NIBIB Interfaces Training Program at UCSD.

Sources of Funding

This work was funded by the Veteran's Affairs Medical Research Department (P.D.L), by the National Institute of Health grants NS/043300, and NS/052565 (P.D.L.), NS/041096, and EB\003832 (D.K.).

Disclosure

None.

References

1. Hawkins BT, Davis TP. The blood-brain barrier/neurovascular unit in health and disease. *Pharmacol Rev*. 2005;57:173–185.
2. Latour LL, Kang DW, Ezzeddine MA, Chalela JA, Warach S. Early blood-brain barrier disruption in human focal brain ischemia. *Ann Neurol*. 2004;56:468.
3. Lo EH, Dalkara T, Moskowitz MA. Mechanisms, challenges and opportunities in stroke. *Nat Rev Neurosci*. 2003;4:399–415.
4. Figueroa BE, Keep RF, Betz AL, Hoff JT. Plasminogen activators potentiate thrombin-induced brain injury. *Stroke*. 1998;29:1202.
5. Jackson-Friedman C, Lyden PD, Nunez S, Jin A, Zweifler R. High dose baclofen is neuroprotective but also causes intracerebral hemorrhage: A quantal bioassay study using the intraluminal suture occlusion method. *Exp Neurol*. 1997;147:346.
6. Bederson JB, Pitts LH, Tsuji M, Nishimura MC, Davis RL, Bartkowski H. Rat middle cerebral-artery occlusion - evaluation of the model and development of a neurologic examination. *Stroke*. 1986;17:472.
7. Longa EZ, Weinstein PR, Carlson S, Cummins R. Reversible middle cerebral artery occlusion without craniectomy in rats. *Stroke*. 1989; 20:84.
8. Tsai PS, Friedman B, Ifarraguerri AI, Thompson BD, Lev-Ram V, Schaffer CB, Xiong Q, Tsien RY, Squier JA, Kleinfeld D. All-optical histology using ultrashort laser pulses. *Neuron*. 2003;39:27–41.
9. Nguyen QT, Tsai PS, Kleinfeld D. Mpscope: A versatile software suite for multiphoton microscopy. *J Neurosci Methods*. 2006;156:351–359.
10. Weibel ER. *Stereological methods: Practical methods for biological morphometry*. San Diego: Academic Press; 1989:volume 1.
11. Thorball N. Fitc-dextran tracers in microcirculatory and permeability studies using combined fluorescence stereo microscopy, fluorescence light microscopy, and electron microscopy. *Histochemistry*. 1981;71: 209–233.
12. Nagaraja TN, Keenan KA, Fenstermacher JD, Knight RA. Acute leakage patterns of fluorescent plasma flow markers after transient focal cerebral ischemia suggest large openings in blood-brain barrier. *Microcirculation*. 2008;15:1–14.
13. Friedman B, Schachtrup C, Tsai PS, Shih AY, Akassoglou K, Kleinfeld D, Lyden PD. Acute vascular disruption and aquaporin 4 loss after stroke. *Stroke*. 2009;40:2182–2190.
14. Brightman MW, Klatzo I, Olsson Y, Reese TS. The blood-brain barrier to proteins under normal and pathological conditions. *J Neurol Sci*. 1970; 10:215–239.
15. Yang GY, Betz AL. Reperfusion-induced injury to the blood-brain barrier after middle cerebral artery occlusion in rats. *Stroke*. 1994;25:1658.
16. Ennis SR, Keep RF, Schielke GP, Betz AL. Decrease in perfusion of cerebral capillaries during incomplete ischemia and reperfusion. *J Cereb Blood Flow Metab*. 1990;10:213–220.
17. Sage JI, Van Uitert RL, Duffy TE. Early changes in blood brain barrier permeability to small molecules after transient cerebral ischemia. *Stroke*. 1984;15:46–50.
18. Hossmann KA, Olsson Y. Influence of ischemia on the passage of protein tracers across capillaries in certain blood-brain barrier injuries. *Acta Neuropathol*. 1971;18:113–122.

19. Rosenberg GA, Estrada E, Dencoff JE. Matrix metalloproteinases and TIMPs are associated with blood-brain barrier opening after reperfusion in rat brain. *Stroke*. 1998;29:2189.
20. Steinwall O, Klatzo I. Selective vulnerability of the blood-brain barrier in chemically induced lesions. *J Neuropathol Exp Neurol*. 1966;25: 542–559.
21. Belayev L, Busto R, Zhao W, Ginsberg MD. Quantitative evaluation of blood-brain barrier permeability following middle cerebral artery occlusion in rats. *Brain Res*. 1996;739:88.
22. Dawson DA, Ruetzler CA, Hallenbeck JM. Temporal impairment of microcirculatory perfusion following focal cerebral ischemia in the spontaneously hypertensive rat. *Brain Res*. 1997;749:200–208.
23. Neumann-Haefelin T, Kastrup A, de Crespigny A, Yenari MA, Ringer T, Sun GH, Moseley ME. Serial mri after transient focal cerebral ischemia in rats. *Stroke*. 2000;31:1965.
24. Huber JD, Egleton RD, Davis TP. Molecular physiology and pathophysiology of tight junctions in the blood-brain barrier. *Trends Neurosci*. 2001;24:719.
25. Cipolla MJ, Crete R, Vitullo L, Rix RD. Transcellular transport as a mechanism of blood- brain barrier disruption during stroke. *Front Biosci*. 2004;9:777–785.
26. Lossinsky AS, Shivers RR. Structural pathways for macromolecular and cellular transport across the blood-brain barrier during inflammatory conditions. *Review Histol Histopathol*. 2004;19:535–564.
27. Hamann GF, Okada Y, Fitridge R, del Zoppo GJ. Microvascular basal lamina antigens disappear during cerebral ischemia and reperfusion. *Stroke*. 1995;26:2120–2126.
28. Maier CM, Hsieh L, Yu F, Bracci P, Chan PH. Matrix metalloproteinase-9 and myeloperoxidase expression: Quantitative analysis by antigen immunohistochemistry in a model of transient focal cerebral ischemia. *Stroke*. 2004;35:1169–1174.
29. Asahi M, Wang X, Mori T, Sumii T, Jung JC, Moskowitz MA, Fini ME, Lo EH. Effects of matrix metalloproteinase-9 gene knock-out on the proteolysis of blood-brain barrier and white matter components after cerebral ischemia. *J Neurosci*. 2001;21:7724–7732.
30. Heo JH, Lucero J, Abumiya T, Koziol JA, Copeland BR, del Zoppo GJ. Matrix metalloproteinases increase very early during experimental focal cerebral ischemia. *J Cereb Blood Flow Metab*. 1999;19:624.
31. Hosomi N, Lucero J, Heo JH, Koziol JA, Copeland BR, del Zoppo GJ. Rapid differential endogenous plasminogen activator expression after acute middle cerebral artery occlusion. *Stroke*. 2001;32:1341–1348.
32. Tagaya M, Haring HP, Stuiver I, Wagner S, Abumiya T, Lucero J, Lee P, Copeland BR, Seiffert D, del Zoppo GJ. Rapid loss of microvascular integrin expression during focal brain ischemia reflects neuron injury. *J Cereb Blood Flow Metab*. 2001;21:835.
33. Sharp FR, Lu A, Tang Y, Millhorn DE. Multiple molecular penumbras after focal cerebral ischemia. *J Cereb Blood Flow Metab*. 2000;20:1011.

Acknowledgements

Chapter 2, in full, is a reprint of the material as it appears in

Chen B, Friedman B, Cheng Q, Tsai P, Schim E, Kleinfeld D, Lyden PD. Severe blood-brain barrier disruption and surrounding tissue injury. Stroke. 2009 Dec;40(12):e666-74.

Permission was obtained from co-authors. I am the primary researcher and author of this paper.

III. THROMBIN MEDIATES SEVERE NEUROVASCULAR INJURY DURING ISCHEMIA

Introduction

Cerebral ischemia triggers several inter-related events, including cytotoxic and vasogenic edema, microvascular thrombosis, and tissue degeneration[7, 9, 65-66]. Although the molecular mechanisms of cellular death in ischemia have not been fully understood, blood-brain barrier leakage of serum constituents might exert a direct toxic effect on brain parenchyma[67-69]. Previous research has identified several candidate toxic factors, such as plasmin, tissue plasminogen activator (tPA), fibrin, fibrinogen, and thrombin, most of which are components involved in blood clotting and clot lysis[70]. Blood-brain barrier breakdown allows the entry of these toxic factors, normally excluded from the brain, to the parenchymal tissue and cause severe damage.

Blood-derived toxic factors

Among all the serum constituents, tPA is one of the best-studied proteases in the central nervous system. Circulating tPA has a short half-life of 5-8 min, and the activity of tPA is restricted by plasminogen activator inhibitor-1 (PAI-1). In the presence of fibrin, tPA is unaffected by PAI-1, and instead will activate the zymogen plasminogen into plasmin, which mediates fibrinolysis and dissolves clots. Clinically, administration of tPA beyond the 4.5 hour window is not beneficial to patients and treatment beyond 8 hours is associated with increased risk of hemorrhagic transformation. In rodent models, plasminogen activation could be detected after 3hr of ischemia and persists for as long as seven days[71-72]. Excessive tPA in central nervous system has been related to

increased neuronal damage, possibly through the excitotoxicity of NMDA receptor[73-74].

Plasmin, converted by tPA from its zymogen form plasminogen, is a potential toxic factor too. *In vitro* studies have showed that plasmin is able to digest components of basement membrane such as fibronectin and laminin[75]. Plasmin could also activate MMP-2 and MMP-9, major extracellular matrix proteins involved in blood-brain barrier permeability during ischemic stroke[76]. *In vivo*, direct injection of high dose plasmin into striatum leads to increased neuronal apoptosis and tissue injury[67].

Fibrinogen is yet another blood-derived factor that could enter parenchymal tissue after blood-brain barrier breakdown and mediate potential toxic effects[77]. In the presence of thrombin, fibrinogen is cleaved into three peptides including fibrinopeptide A and B, and fibrin monomer that subsequently polymerizes to form the insoluble fibrin clot. Fibrinogen is also indicated to interact with several integrins and adhesion proteins that are involved in platelet activation and inflammatory response. Fibrinogen is likely to serve as the anchoring matrix for other membrane surface proteins or growth factors, without exerting direct toxic effects on cells. The *in vivo* role of fibrinogen in disease model remains uncertain.

Although many toxic factors might enter brain via vascular leakage and cause cellular injury, I focus on the role of thrombin in stroke for three main reasons. First, thrombin is one of the earliest mediators responding to vascular

injury and is only activated on the injured sites. Second, the biology of thrombin-induced effects are widely studied *in vitro* and relatively more illuminated than the other candidates. Third, there are powerful anti-thrombin drugs already on the market which will greatly facilitate the experiments.

Thrombin toxicity

Thrombin is a major regulator in the coagulation pathway[78-79]. During endothelial damage or brain trauma, thrombin is activated from the cleavage of prothrombin by Factor X. Thrombin then will convert soluble fibrinogen to fibrin and activate platelets, forming the mesh-work of blood clot[80-82]. The continuous formation of micro-thrombus is likely to exacerbate focal ischemia by occluding the vasculature beyond the initial occlusion sites.

Thrombin has been shown to cause cell death *in vitro*. The direct cytotoxic effects of thrombin appear to be mediated by protease activated receptors (PARs)[83-85], most significantly the PAR1 receptor[86-87]. Activation of PAR1 leads to neuronal cell death, astrocytic proliferation, microglial activation, and toxin release[88-89]. Thrombin could also affect blood-brain barrier integrity by remodeling the endothelial junctional proteins. These toxic effects are mostly associated with high dose thrombin. Low dose thrombin, however, could be neuroprotective and promote angiogenesis and neurogenesis.

Thrombin toxicity has also been tested *in vivo*. Direct injection of high doses of thrombin (5U-25U) in the brain causes significant tissue injury and

edema[90-95]. In hemorrhagic stroke models, continuous release of activated thrombin from existing clots causes severe damage to the brain tissue[96], while infusion of argatroban, a direct inhibitor of thrombin, showed a reduced level of peri-hematomal infarction[97-99]. These data suggested that thrombin is a likely candidate to mediate vascular and tissue injury following stroke.

We sought to determine whether thrombin mediated endothelial barrier dysfunction and tissue injury using an *in vivo* ischemia model.

Materials and Methods

All protocols were approved by the Animal Research Committee of the Veteran's Affairs Medical Center, San Diego, and by the IACUC of University of California San Diego, following all national guidelines for the care of experimental animals.

Animal model

The procedure for middle cerebral artery occlusion (MCAo) model was performed as described previously by the Lyden lab[100-101].The subjects were male adult Sprague Dawley rats, 290g to 310g. All animals received tail-vein injections of 0.3mL FITC-dextran (Sigma-Aldrich, FD2000S; 2MDa, 5% solution in phosphate buffered saline) at the start of the surgery[1]. Animals were anesthetized with 4% isoflurane mixed in oxygen and nitrous oxide (30:70) by facemask. A midline neck incision was made exposing the left common carotid artery. The external carotid and pterygopalatine arteries were ligated with 4-0 silk. An incision was made in the wall of the external carotid artery close to the bifurcation point of the external and internal carotid arteries. A 4–0 heat-blunted nylon suture (Ethicon) was then inserted and advanced approximately 17.5 mm from the bifurcation point into the internal carotid arteries, thereby blocking the ostium of the middle cerebral artery. The suture was removed later, typically after 4 hours but this could be varied, to allow the reperfusion of blood flow for 30 minutes. To avoid the complexity of laser Doppler flow monitoring, which requires scalp retraction and burr hole placement, we used clinical ratings to assure

proper placement of the nylon filament. Neurological abnormality was examined 1 hour after ischemia onset and again during reperfusion using a published rodent neurological grading system[102]. Typically animals with 3 positive findings (abnormal forepaw retraction on tail lift, circling, reduced exploration, obvious hemiparesis) on both the 1-hour and the reperfusion examinations were found to have lesions; animals with fewer findings were typically excluded. Animals were excluded also for subarachnoid hemorrhage found at postmortem dissection. At the end of the reperfusion period, animals were euthanized with an overdose of pentobarbital and then intracardially perfused with 250 ml saline followed by 300 ml of 4% paraformaldehyde. Brains were removed, post-fixed, cryoprotected in 30% sucrose, and then sliced into 50μm sections on a freezing microtome (Reichert-Jung).

Drug preparation

Subjects were randomly assigned each day to receive thrombin or vehicle (saline) and then all laboratory staff remained blind to group assignment until the code was unmasked after all data analysis was complete. Rat thrombin (Sigma-Aldrich, T5772) was dissolved in saline at 1unit/ml and infused through PE10 tubing attached to the external carotid artery immediately after the onset of MCA occlusion. The infusion continued using a syringe pump (Thermo Scientific, Orion M362) at 0.2mL/hr for 4hr ischemia and 30min reperfusion. Argatroban (Enzo Life Sciences, BML-PI146) was dissolved in saline at 0.56mg/ml and was infused through jugular vein using a syringe pump. We started to infuse argatroban

(1.69mg/kg) immediately after the onset of ischemia and continued for the duration of ischemia and reperfusion. Dosage of argatroban was based on published results[98].

Immunofluorescence of thrombin

Sections were immunostained with primary antibodies including goat anti-thrombin (Santa Cruz, sc-23335, 1:200), mouse anti-NeuN (Millipore, MAB377, 1:1000), mouse anti-GFAP (Millipore, MAB360, 1:5000), and fluorescent secondary antibodies Cy5 anti-goat IgG (Millipore, AP180S, 1:1000), Cy3 anti-mouse IgG (Millipore, AP192C, 1:1000). The protocol for immunostaining is described in brief: sections were permeabilized with 5% bovine serum albumin and 0.1% triton X-100 for 1 hour, incubated with primary antibody at 4°C for 2 days, and followed by incubation with secondary antibody at room temperature for 4 hours. Sections were washed in PBS, mounted on slides, and cover-slipped with Pro-Long antifade reagent (Invitrogen). To confirm the specificity of thrombin antibody, three control experiments were conducted using no primary antibody, primary antibody pre-incubated with blocking peptide (Santa Cruz, sc-23335P), and primary antibody pre-incubated with rat plasma thrombin (Sigma-Aldrich, T5772). Fluorescent images were obtained using confocal microscopy (Olympus FV1000).

Analysis of vascular damage

To characterize the extent of severe blood-brain barrier disruption in each animal, 9 sections spanning the MCA territory were imaged under epi-fluorescence microscopy using a highly sensitive CCD camera (Apogee, KAF32MB). The signal of FITC-dextran was quantified using Image-Pro Plus (Cybermedia) as described previously[1]. To characterize the extent of blood-brain barrier opening—which is different from severe vascular disruption—sections were processed for immunostaining of endogenous IgG. Briefly, sections were quenched in 3% hydrogen peroxide for 10 minutes, incubated in primary antibody at 4°C for 1 day (Vector Laboratories, anti-universal IgG), and then incubated in biotinylated anti-rabbit secondary antibody for 4 hours, followed by peroxidase catalysis of diaminobenzidine reporter (Vector Laboratories, PK6100 and SK4100). The distribution of IgG was outlined and quantified using Image-Pro Plus using methods previously published[1].

Cell death assay

To detect the cellular death associated with ischemic vascular disruption, a TUNEL staining protocol was employed using the In Situ Cell Death Detection Kit (Roche, Cat# 12156792) with minor modification. Sections prepared above were pretreated with fresh 0.1% Triton X-100 and 0.1% sodium citrate buffer for 10 minutes on ice. Then the sections were rinsed twice with phosphate buffered saline (PBS), and incubated with TUNEL reaction mixture prepared according to the manufacturer's instruction for 3 hours at 37ºC. Finally, the sections were

rinsed in PBS, mounted with ProLong Gold antifade reagent (Invitrogen), and imaged with a stereoscope (Olympus, MVX10 MacroView). Three images spanning the striatum on the ischemic side were recorded for each brain section, and the number of TUNEL positive cells was counted.

Results

Thrombin increased within regions of vascular disruption

Significant staining of thrombin was found in regions of severe vascular disruption labeled by FITC-dextran fluorescence, compared to regions with less or no FITC fluorescence (Fig. 1). Double staining with NeuN or GFAP revealed that most cellular staining of thrombin was associated with neurons, some with astrocytes and microvessel.(Fig. 2).

Thrombin promoted severe vascular disruption

Compared to the vehicle group, the thrombin group showed an increase in the volume of severe vascular disruption, as labeled by the fluorescence of high molecular weight dextran-FITC (Fig. 3A). The areas of vascular damage after thrombin treatment were greater in striatum and extended to most regions of cortex, whereas after vehicle treatment the severe vascular disruption was confined to the striatum (Independent samples *t*-test, $P<0.05$, Fig. 3B). The same brain slices were immunostained with IgG antibody, using DAB as the reporter, to examine the blood-brain barrier leakage of smaller molecular weight plasma proteins (Fig. 3C). The results demonstrated widespread regions of blood-brain barrier permeability across the brain section in the thrombin group compared to the vehicle group (Independent samples *t*-test, $P<0.05$, see, Fig. 3D).

Argatroban protected the brain from ischemic vascular injuries

To determine whether thrombin inhibition could ameliorate severe vascular injury during stroke, subjects were randomly assigned to receive intravenous argatroban or vehicle. In the group receiving argatroban treatment, the average clotting time increased by 30% (data not shown), confirming adequate delivery of the thrombin inhibitor. The brains exhibited a significant reduction in severe vascular disruption, as labeled with high molecular weight FITC-dextran (Fig. 4A). The number of injured blood vessels and the areas of FITC-dextran distribution were reduced by 60% compared to the group receiving vehicles (Independent samples *t*-test, $P<0.05$, Fig. 4B). No cortical vascular damage was observed in the argatroban treatment group. The neurological score after 4 hours MCAo in the argatroban group (2.8±0.3, n=6) was not significantly different from that in the vehicle group (3.0±0.0, n=5).

Argatroban blocked thrombin-mediated vascular disruption

To confirm that the observed ischemic injury to vasculature was mediated in part through thrombin activity, we infused argatroban through jugular vein simultaneously with the arterial infusion of thrombin through the internal carotid artery during ischemia and reperfusion. During arterial infusion of thrombin, 1.69mg/kg argatroban infused intravenously alleviated the vascular disruption, but not to a significant extent. A higher dose of argatroban (3.4mg/kg) significantly reduced severe vascular disruption during MCAo and arterial thrombin infusions ($P<0.01$, ANOVA with Neuman-Keuls, Fig. 5).

Thrombin inhibition reduced neuronal injury

In areas of reduced vascular injury, counts of TUNEL stained cells were significantly reduced after argatroban treatment (Fig. 6). Intra-arterial thrombin increased the extent of TUNEL staining during ischemia. When thrombin was infused into the MCA while argatroban was given intravenously, the numbers of TUNEL positive cells decreased.

Discussion

Our data establish for the first time that thrombin plays a crucial role in causing severe vascular injury during ischemia. Arterial infusions of thrombin augmented the extent of severe vascular injury, while intravenous treatment with the direct thrombin inhibitor argatroban inhibited the effect of thrombin on severe vascular disruption in a dose related manner. Our data, obtained in a well-characterized MCAo model, confirms previous findings from *in vitro* and hemorrhagic models *in vivo* suggesting a cytotoxic property of thrombin. Ischemic cellular injury, represented as counts of TUNEL stained cells, increased with thrombin and decreased with argatroban treatments, confirming that severe vascular injury and cellular damage are both influenced by thrombin activation.

Most likely, thrombin plays multiple roles during cerebral ischemic insult[87]. Despite the deleterious effect discussed above, however, some studies have suggested a beneficial role for thrombin. Low dose thrombin was neuroprotective and was a potent mediator for neurogenesis and angiogenesis[103-107]. Injection of low dose thrombin could also serve to induce brain tolerance to ischemic attack[108-110]. Therefore, it is likely that thrombin effects are dosage dependent. In our experiment, we infused a small amount of thrombin (3units/kg) over 4 hours, a dose that was previously used to precondition the brain against ischemia[109-110]. Interestingly, in the present experiment the infusion of low dose thrombin resulted in severe damage to the brain vasculature, suggesting that intraarterial infused thrombin might undergo an amplification process through the coagulation

cascade[111]. This speculation was supported by the observation that vascular damage by the exogenous thrombin could only be inhibited by a higher dose of argatroban (3.4mg/kg). Since we did not measure intra-arterial clot burden, however, we cannot definitively address this point.

Further studies are essential to define the mechanisms by which thrombin augments ischemic damage. In particular, the role of PAR1 mediated injury seems critical, as well as the role of thrombin mediated micro-thrombosis. Perhaps most importantly, it remains to be determined whether thrombin enters brain parenchyma to cause direct cytotoxic injury, or simply exacerbates blood brain barrier disruption leading indirectly to increased edema and tissue injury.

In summary, thrombin mediates severe vascular disruption during ischemia and thrombin inhibitors may partially ameliorate vascular disruption. Further work is needed to establish whether thrombin, entering parenchyma due to increased vascular permeability, augments neurotoxicity during ischemia.

Figures

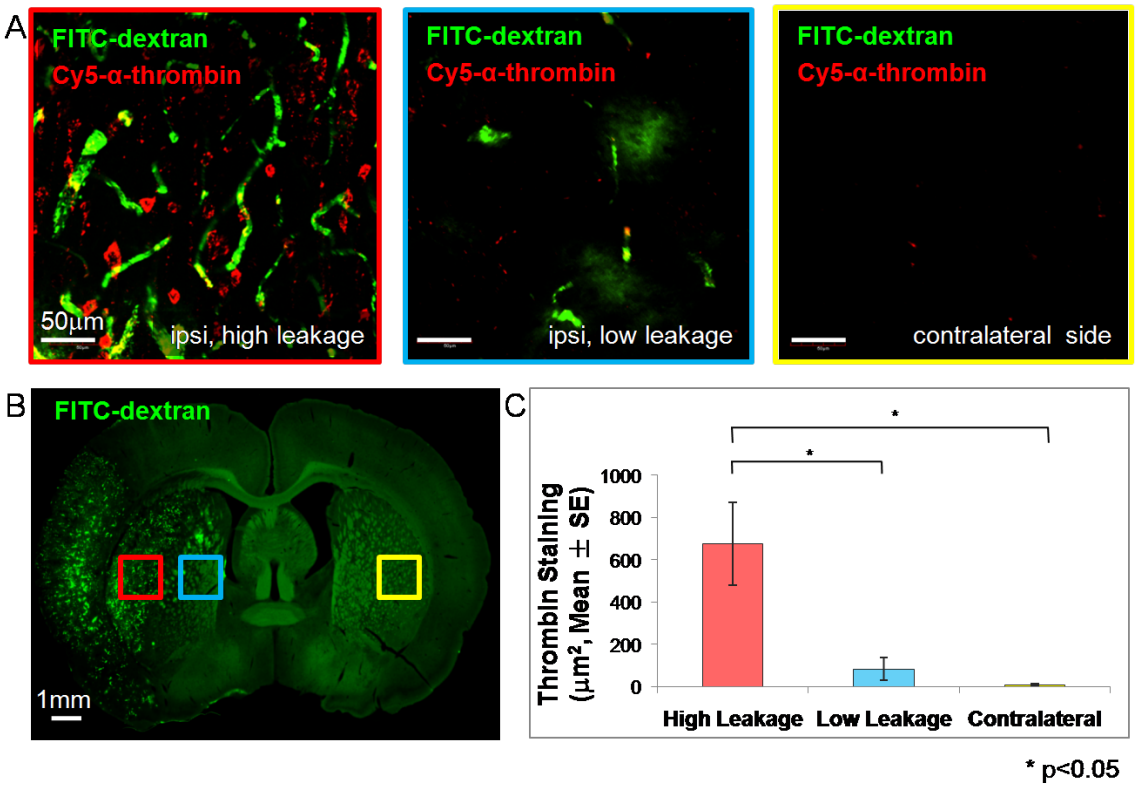

Figure 1. Thrombin accumulated in regions of vascular leakage.

Significant staining of thrombin was found in subregions suffering severe ischemic injury, as labeled by FITC-dextran fluorescence (red frame), compared to regions with lesser extent of ischemia (blue frame) and region without vascular labeling (yellow frame).

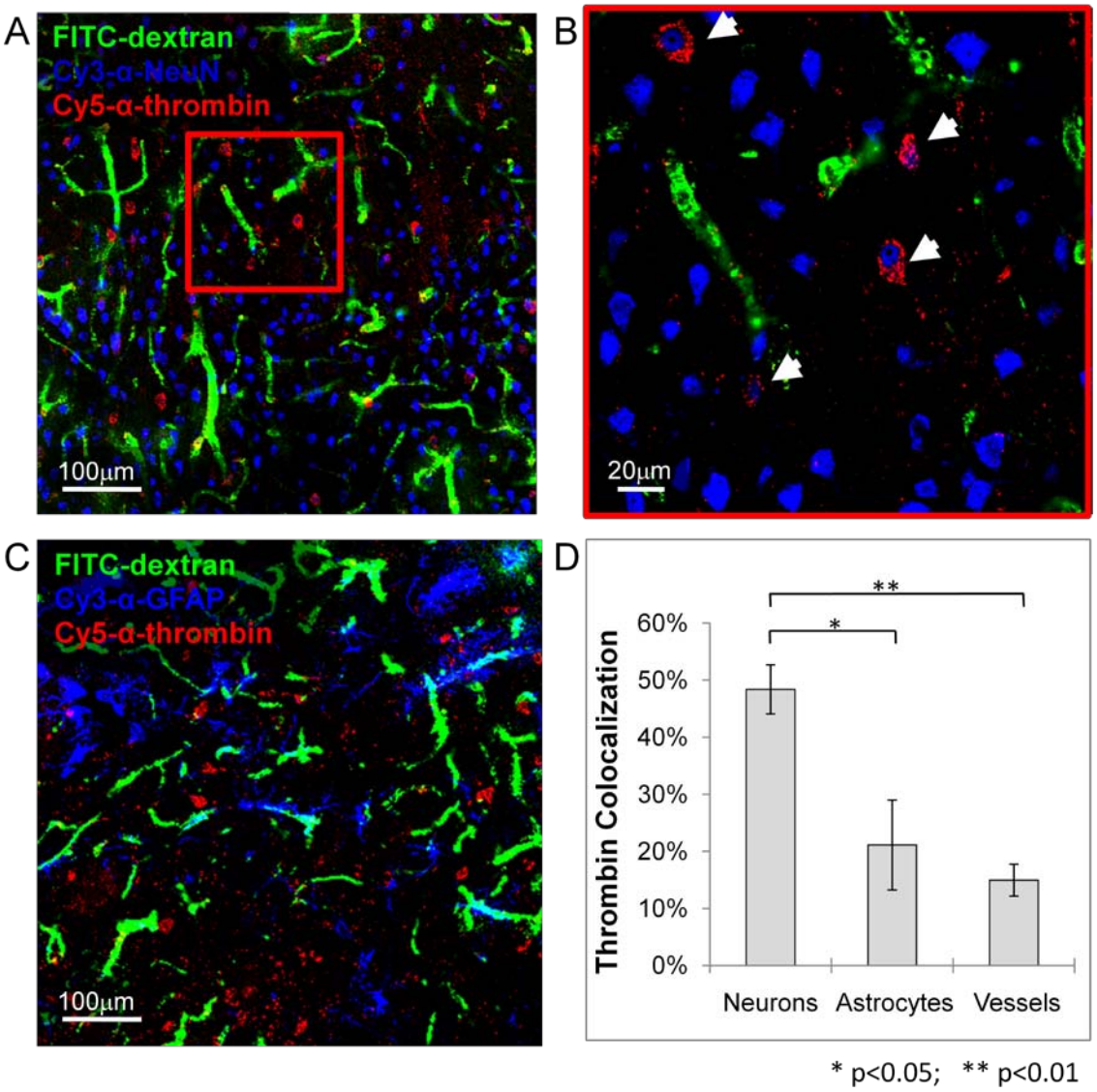

Figure 2. Cell specific binding of thrombin on parenchymal tissue

(A) Double staining with NeuN revealed that most cellular staining of thrombin was associated with neurons as labeled by the neuronal nuclei marker NeuN. The image was taken at 20x objective of Olympus FV1000 Confocol Microscope. (B) Image of high magnification (60x) delineate clear staining of thrombin (red) wrapping the neuronal nuclei (blue). (C) Less thrombin colocalized with GFAP the marker for astrocytes.

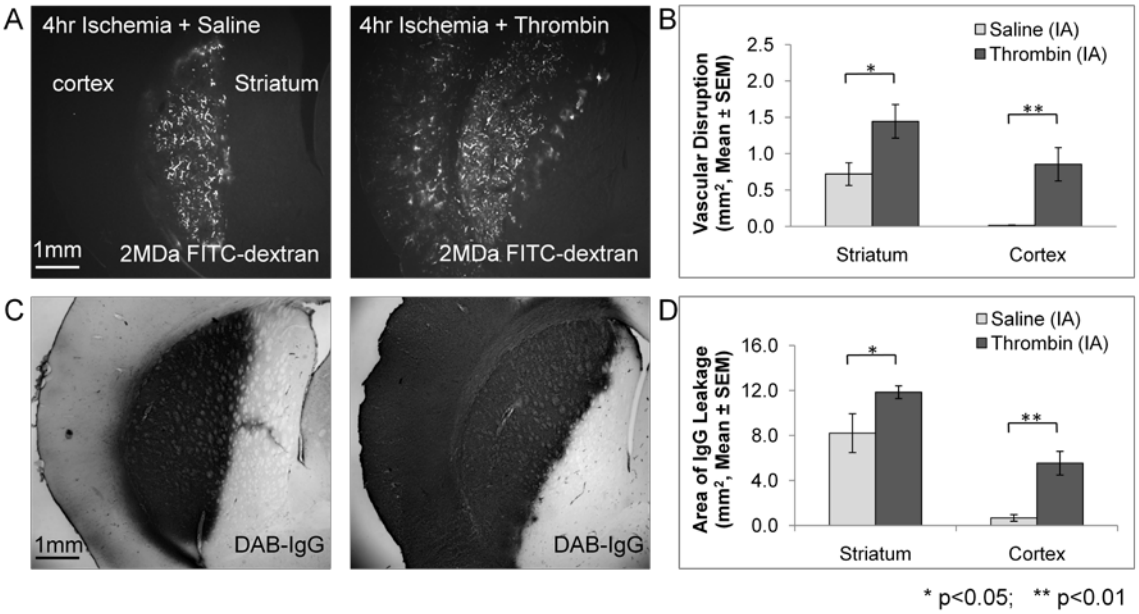

Figure 3. Thrombin promoted vascular disruption during ischemia

(A) Treatment of thrombin during 4hr ischemia greatly enlarged the brain region of severe vascular disruption, as visualized by 2MDa FITC-dextran. (B) The signals of FITC-dextran were quantified using the method previously described[1]. In the thrombin group (n=6) the area of FITC-dextran in both striatum and cortex was larger than in the vehicle group (n=5). (C) Blood-brain barrier leakage, as visualized by IgG, was mostly confined to lateral striatum ipsilateral to the MCA occlusion in the vehicle group, whereas in the thrombin group IgG leakage involved cortex as well. (D) After thrombin treatment, the area of IgG leakage showed increased modestly in striatum and very significantly in cortex. * P<0.05; ** P<0.01.

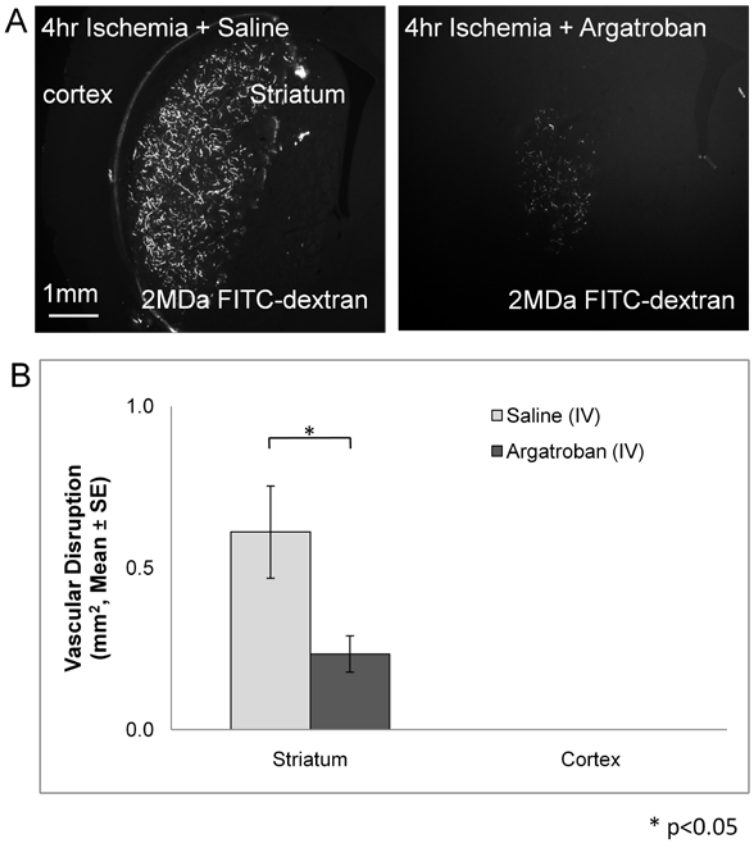

Figure 4. Intravenous infusion of argatroban reduced severe vascular damage during ischemia

(A) Examples of brain slices in argatroban group (right) and vehicle group (left). Treatment with argatroban during ischemia protected the brain from ischemic vascular disruption labeled by FITC-dextran. (B) The area of FITC-dextran distribution was significantly reduced in argatroban group (n=6) compared to the vehicle group (n=5). No cortical vascular damage was found in either group. * P<0.05.

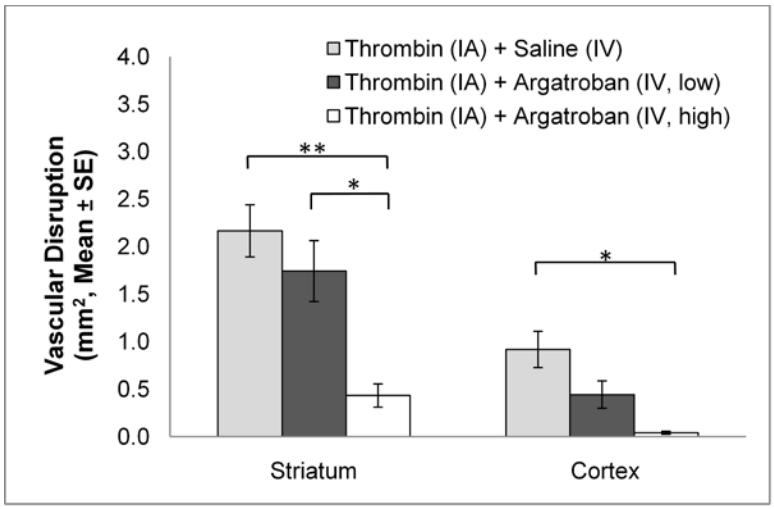

Figure 5. Argatroban blocked thrombin-mediated vascular disruption.

To test the specificity of thrombin toxicity during ischemia, thrombin was infused into the internal carotid artery in all animals during 4hr MCA occlusion, with simultaneous infusion of vehicle or argatroban through the jugular vein. Treatment with argatroban ameliorated thrombin-induced vascular injury in a dose dependent manner (ANOVA, $P<0.01$). * $P<0.05$; ** $P<0.01$.

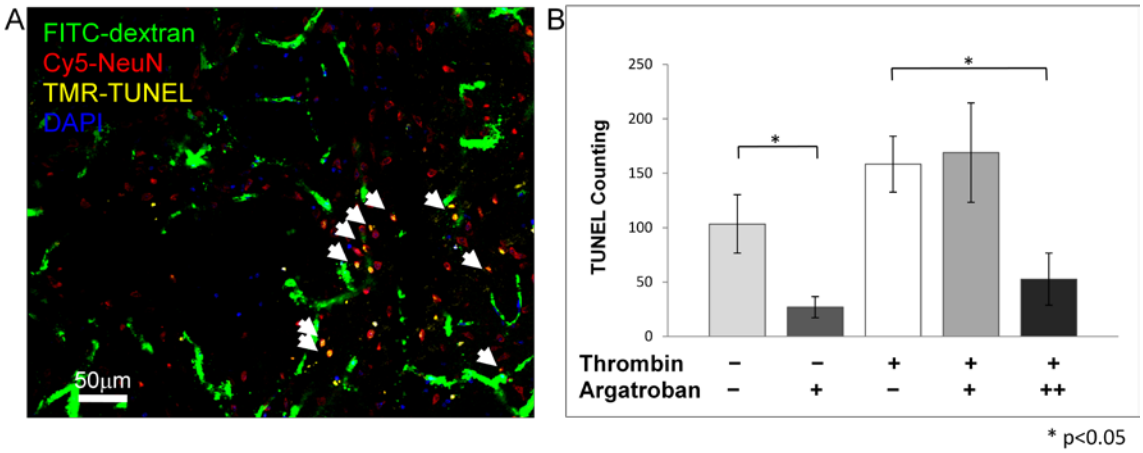

Figure 6. Thrombin inhibition reduced neuronal injury.

(A) Cellular death was identified by TUNEL staining (indicated by the arrow). 70% of the TUNEL positive cells were doubled labeled with NeuN, specific neuronal nuclei marker. (B) Intra-arterial thrombin increased the extent of TUNEL staining during ischemia. When thrombin was infused into the MCA while argatroban was given intravenously, the numbers of TUNEL positive cells significantly decreased ($P<0.05$, Independent Samples *t*-test after Bonferonni correction).

Acknowledgement

Chapter 3, in part, has been submitted for publication of the material as it may appear in

Chen B, Cheng Q, Yang K, Lyden PD. Thrombin mediates severe neurovascular injury during ischemia. Stroke, 2010.

Permission was obtained from co-authors. I am the primary researcher and author of this paper.

IV. PAR1 MEDIATES THROMBIN TOXICITY AFFECTING VASCULAR DISRUPTION AND TISSUE INJURY DURING ISCHEMIA

Introduction

The mechanism of damage to the neurovascular unit caused by thrombin is not well understood. In general, thrombin might exert its toxic effect by three not-mutually exclusive pathways. One is to promote micro-thrombosis in the smaller distal vessels and exacerbate the ischemic condition downstream of the larger arterial occlusion; another is to induce vascular permeability by PAR1/PKC pathways, remodeling the endothelial junctional structure and causing edema[112-114]; finally, thrombin might leak into parenchymal tissues and cause direct cytotoxic effects on glia and neurons via PAR1/MAPK pathways[90-93 86-89].

Thrombin is a key mediator in the coagulation cascade. When endothelial damage occurs during brain trauma or stroke, platelets rapidly accumulate around the injured sites. Circulating thrombin is recruited to the surface of platelets and activates platelets via the PAR receptors (PAR1 for primates and PAR4 for rodents). Activated platelets then will aggregate with each other through glycoprotein IIb-IIIa adhesion molecule and deposit in the injured area of the vasculature. Docked thrombin will continue to cleave fibrinogen to fibrin, resulting in the meshwork of blood clots with platelets.

Thrombin also mediates cellular signaling pathway by a family of receptors called protease activated receptors (PARs). There are four members of PARs: PAR1 is the major mediator for thrombin signal and can be activated in the presence of low concentration of thrombin; PAR4 is also a thrombin receptor but only responds to high dose of thrombin; PAR3 is the cofactor of PAR4; PAR2 is

activated by trypsin and trypsin-like serine proteases including factor VII and X. Among these four receptors, PAR1 is most well studied. It is widely expressed in sensory neurons, glial cells, platelets (in human), and endothelial cells[115]. In human brain, PAR1 is expressed abundantly in astrocytes and moderately in neurons[116]. Thrombin is considered as the main ligand for PAR1, but other proteases, such as factor X, plasmin, matrix metalloproteinase (MMP), and activated protein C (APC), could also activate PAR1 under certain circumstances[117-121].

PAR1 is a G-protein coupled receptor. The extracellular domain of PAR1 contains a cleavage site for thrombin and will be cleaved upon the binding of thrombin. The new N-terminal peptide is tethered to itself and activates the downstream pathways. Activated PAR1 is rapidly desensitized by phosphorylation and arrestin binding; it is then uncoupled from G protein, internalized, and sorted to lysosome for degradation[115, 117].

Previous studies have indicated that thrombin can act on endothelial cells and disrupt the barrier function. Thrombin activates PAR1 receptors that are associated with Gα 12/13 and Gα11/q, leading to the upregulation of calcium and activation of RhoA/PKC pathways. These actions will affect the remodeling of adherent junction proteins in the endothelial cells and induce endothelial permeability[112]. In addition, thrombin can also activates MMP2 in human microvascular endothelial cells[122]. Most of these investigations were conducted in

cultured endothelial cells and the relevance of these pathways i*n vivo* remains to be clarified.

Thrombin toxicity in the brain can also be mediated by PAR1 signaling in the parenchymal tissue. PAR1 knock-out mice are more resistant to short ischemic insult, and intracerebroventricular injection of a PAR1 antagonist reduces the infarct size as well[86]. Among many cellular signaling pathways induced by PAR1 activation, the mitogen-activated protein kinase (MAPK) appears as an important mediator of thrombin toxicity. The presence of either thrombin or PAR1 agonist in the media can induce a robust response of MAPK phosphorylation in the cultured cells[123-124]. In addition, direct injection of thrombin to the striatum causes severe edema and neuronal injury, which can be alleviated by the co-injection of chemical inhibitors targeted to MAPK kinases p38, ERK, and JNK[91]. Previous studies have implicated a critical role for MAPK signal transduction in cerebral ischemic damage[125].

The mechanism of how thrombin toxicity is mediated in the brain remains unclear. In this study, we will target different components in both coagulation cascade and PAR1/MAPK pathway and test if pharmacological interference of these components will affect the stroke outcome.

Materials and Methods

All protocols were approved by the Animal Research Committee of the Veteran's Affairs Medical Center, San Diego, and by the IACUC of University of California San Diego, following all national guidelines for the care of experimental animals.

Animal model

The procedure for middle cerebral artery occlusion (MCAo) model was performed as described previously[100-101].The subjects were male adult Sprague Dawley rats, 290g to 310g. All animals received tail-vein injections of 0.3mL FITC-dextran (Sigma-Aldrich, FD2000S; 2MDa, 5% solution in phosphate buffered saline) at the start of the surgery[1]. Animals were anesthetized with 4% isoflurane mixed in oxygen and nitrous oxide (30:70) by facemask. A midline neck incision was made exposing the left common carotid artery. The external carotid and pterygopalatine arteries were ligated with 4-0 silk. An incision was made in the wall of the external carotid artery close to the bifurcation point of the external and internal carotid arteries. A 4–0 heat-blunted nylon suture (Ethicon) was then inserted and advanced approximately 17.5 mm from the bifurcation point into the internal carotid arteries, thereby blocking the ostium of the middle cerebral artery. The suture was removed later, typically after 4 hours but this could be varied, to allow the reperfusion of blood flow for 30 minutes. To avoid the complexity of laser Doppler flow monitoring, which requires scalp retraction and burr hole placement, we used clinical ratings to assure proper placement of

the nylon filament. Neurological abnormality was examined 1 hour after ischemia onset and again during reperfusion using a published rodent neurological grading system[102]. Typically animals with 3 positive findings (abnormal forepaw retraction on tail lift, circling, reduced exploration, obvious hemiparesis) on both the 1-hour and the reperfusion examinations were found to have lesions; animals with fewer findings were typically excluded. Animals were excluded also for subarachnoid hemorrhage found at postmortem dissection. At the end of the reperfusion period, animals were euthanized with an overdose of pentobarbital and then intracardially perfused with 250 ml saline followed by 300 ml of 4% paraformaldehyde. Brains were removed, post-fixed, cryoprotected in 30% sucrose, and then sliced into 50μm sections on a freezing microtome (Reichert-Jung).

Drug preparation

Subjects were randomly assigned each day to receive drugs or vehicle and then all laboratory staff remained blind to group assignment until the code was unmasked after all data analysis was complete. The infusion of drugs was started immediately after the onset of MCA occlusion and continued using a syringe pump (Thermo Scientific, Orion M362) at 0.2mL/hr for 4hr ischemia and 30min reperfusion. PAR1 antagonist SCH79797 (Tocris Bioscience, Cat# 1592) was dissolved in DMSO at 8.3mg/mL as 1000x stocking solution, and was diluted in saline and infused into jugular vein at the final concentration of 8.3ug/mL, following the optimal dose as previously reported[126]. MAPK p38 antagonist

SB203580 (Tocris Bioscience, Cat#1402) was dissolved in saline at 4.6ug/mL and infused into jugular vein[91, 93]. The glycoprotein IIb-IIIa inhibitor GR144053 (Tocris Bioscience, Cat#1263) was dissolved in saline at 1.5mg/mL and infused into jugular vein[127-129]. PAR1 agonist peptide TFLLR (Tocris Bioscience, Cat#1464) was dissolved in double distilled water at 450umol/L and infused into internal carotid artery[130-131]. The control peptide RLLFT (Tocric Bioscience, Cat#3393) was prepared in the same diluents at the same concentration.

Immunohistochemistry

At the end of the reperfusion period, animals were euthanized with an overdose of pentobarbital and then intracardially perfused with 250 ml saline followed by 300 ml of 4% paraformaldehyde. Brains were removed, post-fixed, cryoprotected in 30% sucrose, and then sliced into 50μm sections on a freezing microtome (Reichert-Jung). Sections were immunostained with primary antibodies goat anti-thrombin (Santa Cruz, sc-23335, 1:200), rabbit anti-PAR1 (H-111, Santa Cruz, sc-5605, 1:200), mouse anti-NeuN (Millipore, MAB377, 1:1000), mouse anti-GFAP (Millipore, MAB360, 1:5000), mouse anti-CD31 (Millipore, CBL468, 1:300). Selective Cy3 or Cy5 conjugated secondary antibodies were obtained from Millipore. The protocol for immunostaining is described in brief: sections were permeabilized with 5% bovine serum albumin and 0.1% triton X-100 for 1 hour, incubated with primary antibody at 4°C for 2 days, and followed by incubation with secondary antibody at room temperature

for 4 hours. Sections were washed in PBS, mounted on slides, and cover-slipped with Pro-Long antifade reagent (Invitrogen).

Cell death assay

To detect the cellular death associated with ischemic vascular disruption, a TUNEL staining protocol was employed using the In Situ Cell Death Detection Kit (Roche, Cat# 12156792) with minor modification. Sections prepared above were pretreated with fresh 0.1% Triton X-100 and 0.1% sodium citrate buffer for 10 minutes on ice. Then the sections were rinsed twice with phosphate buffered saline (PBS), and incubated with TUNEL reaction mixture prepared according to the manufacturer's instruction for 3 hours at 37ºC. Finally, the sections were rinsed in PBS, mounted with ProLong Gold antifade reagent (Invitrogen), and imaged with a stereoscope (Olympus, MVX10 MacroView).

Imaging and quantitative analysis

To characterize the extent of severe blood-brain barrier disruption in each animal, 9 sections spanning the MCA territory were imaged under epi-fluorescence microscopy using a highly sensitive CCD camera (Apogee, KAF32MB). The signal of FITC-dextran was quantified using Image-Pro Plus (Cybermedia) as described previously[1]. To evaluate the extent of cellular death labeled by TUNEL staining, three images spanning the striatum on the ischemic side were recorded for each brain section, and the number of TUNEL positive cells was counted.

Results

PAR1 activation colocalized with vascular leakage of FITC-dextran

Sections from 4hr ischemia brain were immunostained with PAR1 antibody to determine if PAR1 activation occurs in regions of vascular leakage. PAR1 antibody (H-111) targets to the thrombin binding sites on the N-terminal extracellular domain[132-133]. Upon activation, PAR1 is rapidly internalized and degraded. Therefore the activation of PAR1 is evident by the loss of PAR1 antigen signal[134-135]. In sub-regions of severe vascular disruption labeled by FITC-dextran, PAR1 signal were significantly reduced compared to sub-regions with no FITC-dextran fluorescence (Fig. 1).

PAR1 agonist promoted severe vascular disruption and tissue injury

To determine if PAR1 activation mediates thrombin induced vascular disruption during ischemia, we infused PAR1 agonist peptide, TFLLR, through internal carotid artery to the brain for the duration of 4hr ischemia and reperfusion. A scramble sequence peptide RLLFT was employed as a control substance. The group receiving agonist peptide showed 50% increase in the area of FITC-dextran leakage compared to the control group (Independent sample *t*-test, $P<0.05$, Fig. 2A). The number of TUNEL positive cells in the agonist group was also greater than that in the control group (Fig. 2B).

Inhibition of PAR1 reduced brain regions of vascular disruption

We next sought to ask if PAR1 inhibition would block the thrombin toxicity. SCH79797 a novel PAR1 antagonist was infused through jugular vein over 4hr ischemia and 30min reperfusion. Animals were assigned randomly to the treatment group and the control group. The average area of severe vascular disruption in the treatment group was significantly lower than that in the control group (Independent sample *t*-test, $P<0.05$, Fig. 3A). The number of TUNEL positive cells was also significantly reduced ($P<0.05$, Fig. 3B).

Inhibition of p38 kinase activity reduced ischemic injury

To determine whether PAR1 mediated thrombin toxicity is dependent on MAPK kinases during ischemia, we infused SB203580, an antagonist to p38. SB203580 was infused through jugular vein at doses of 1nmol, 5nmol, and 10nmol. The reduction of severe vascular damage was maximal when animals were treated with 10nmol of SB203580 (Fig. 4A). The area of FITC-dextran distribution was significantly less in the treatment group than in the vehicle group (Independent sample *t*-test, $P<0.05$). The number of TUNEL positive cells in the agonist group was also reduced (Fig. 4B).

Inhibition of platelet aggregation did not affect ischemic vascular disruption

To examine if increased coagulation activity contributes to thrombin toxicity on the vasculature during ischemia, we infused GR144053 an inhibitor of platelet aggregation directed against platelet glycoprotein IIb-IIIa during 4hr

ischemia and reperfusion. The overall coagulation activity was significantly increased in the treatment group compared to the vehicle group (Independent sample *t*-test, $P<0.05$; Fig. 5A). However, no significant difference was found in the area of severe vascular disruption between the two groups ($P>0.05$; Fig. 5B). The number of TUNEL positive cells in the treatment group was not significantly different from that in the control group ($P>0.05$; Fig. 5C).

Discussion

We investigated two putative mechanisms of thrombin toxicity during cerebral ischemia. First, we demonstrated that ischemic brain injury by thrombin was in part mediated by PAR1 pathways. PAR1 activation was significantly promoted in regions of severe vascular disruption labeled by FITC-dextran. Arterial infusion of PAR1 agonist peptide mimicked the effect of thrombin on both vasculature and tissue damage, while infusion of PAR1 antagonist ameliorated the ischemic injury. In addition, infusion of a p38 MAPK inhibitor reduced severe vascular damage as well as cell death labeled by TUNEL staining.

We also investigated if the coagulation pathway contributes to thrombin toxicity in our stroke model. Using an inhibitor of platelet aggregation, we were able to interfere in coagulation activity as confirmed by the significant increase in bleeding time. No significant difference was found in either vascular disruption or cell death between treatment group and vehicle group. These results suggested that thrombin toxicity over extended ischemia may not involve a pro-coagulant effect. Inhibitors targeted to other components in coagulation cascade need to be tested in the future studies to confirm this inference.

The exact mechanism how PAR1 activation mediates severe vascular and tissue damage remains elusive. PAR1 expression can be detected in most cell types in the brain but is most abundant in astrocytes and neurons. It is likely that PAR1 participates in diverse cellular activities in different cell types[89, 113, 136]. In neurons, PAR1 activation could lead to reduced neurite growth and apoptosis. In

astrocytes, PAR1 could induce gliosis and toxin release. In endothelial cells, PAR1 could mediate junctional protein remodeling and directly affect the integrity of blood-brain barrier. More recently, a new mechanism involving cell-cell crosstalk was proposed, suggesting that PAR1 activation might mediate glutamate release from astrocytes and result in excitotoxicity in neurons[137-138]. Other PAR1 related cellular responses include activation of microglial cells, generation of reactive oxygen species[139], and release of inflammatory mediators[140]. All of these mechanisms are not mutually exclusive and can potentially contribute to the ischemic damage mediated by thrombin/PAR1 pathway. Further investigation into the mechanism should dissect PAR1 pathway at different cell types in the context of ischemic stroke.

Figures

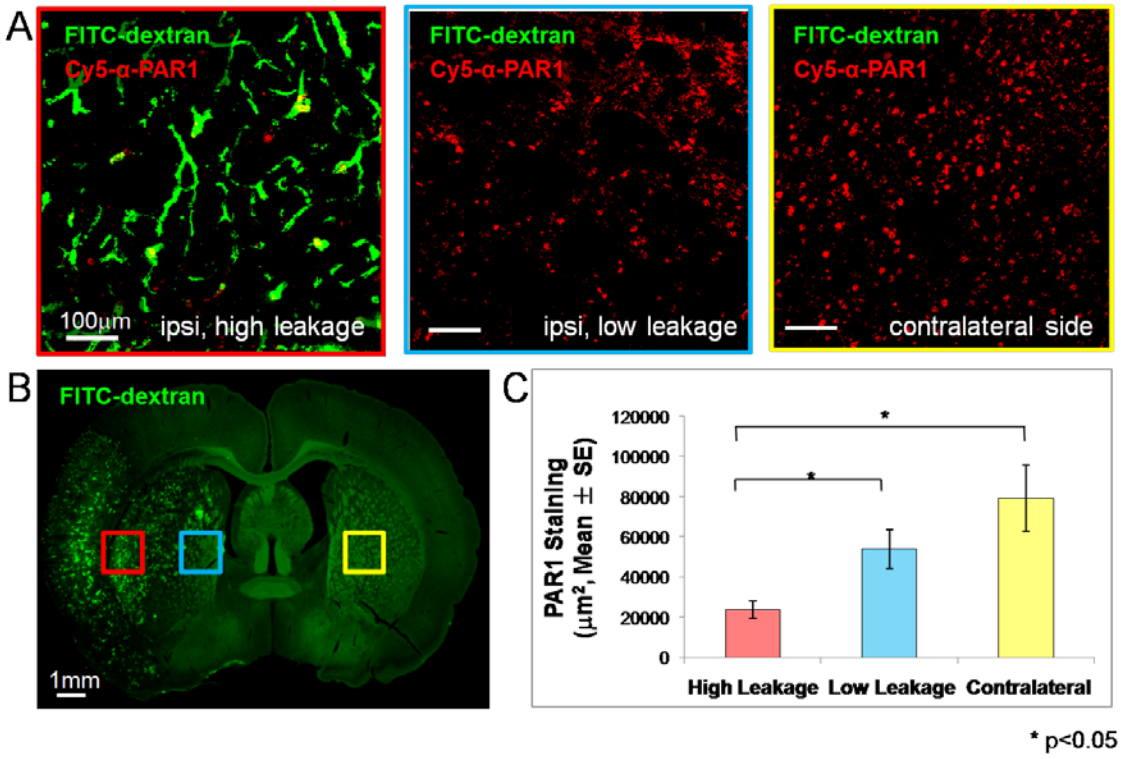

Figure 1. PAR1 activation in regions of vascular leakage

Sections from 4hr ischemia brain were immunostained with PAR1 antibody to determine if PAR1 activation occurs in regions of vascular leakage. In sub-regions of severe vascular disruption labeled by FITC-dextran, PAR1 signal were significantly reduced (red frame) compared to sub-regions with no FITC-dextran fluorescence (blue and yellow frames).

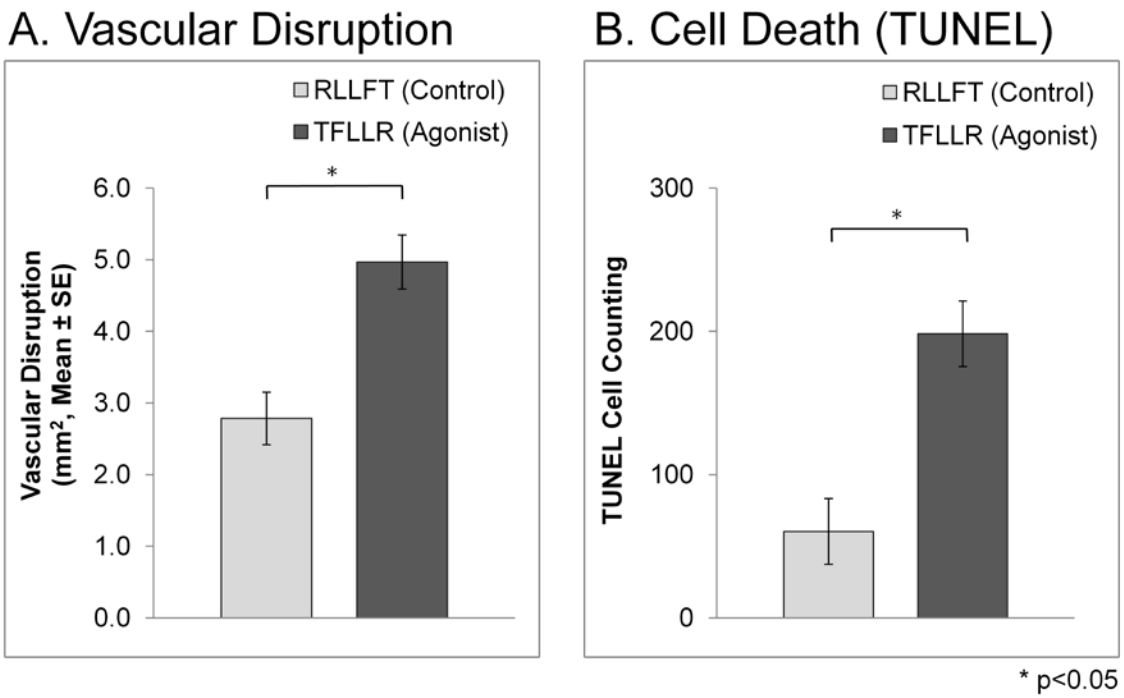

Figure 2. PAR1 agonist promoted vascular disruption and tissue injury

To determine if PAR1 activation mediates thrombin induced vascular disruption during ischemia, we infused PAR1 agonist peptide, TFLLR, through internal carotid artery to the brain for the duration of 4hr ischemia and reperfusion. A ramble sequence peptide RLLFT was employed as a control substance. (A) The group receiving agonist peptide showed 50% increase in the area of FITC-dextran leakage compared to the control group (Independent sample t-test, *P<0.05*). (B) The number of TUNEL positive cells in the agonist group was also greater than that in the control group (Independent sample t-test, *P<0.05*).

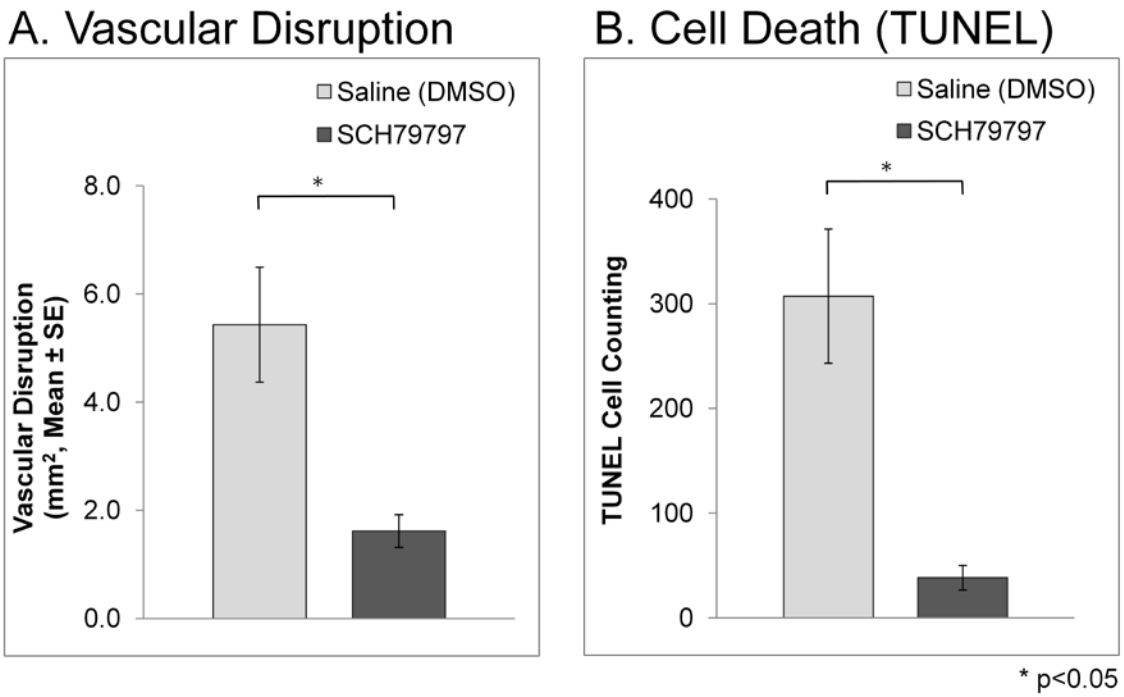

Figure 3. Inhibition of PAR1 reduced areas of vascular disruption and cell death

SCH79797 a novel PAR1 antagonist was infused through jugular vein over 4hr ischemia and 30min reperfusion. Animals were assigned randomly to the treatment group and the control group. (A) The average area of severe vascular disruption in the treatment group was significantly lower than that in the control group (Independent sample t-test, *P<0.05*). (B) The number of TUNEL positive cells was also significantly reduced (*P<0.05*).

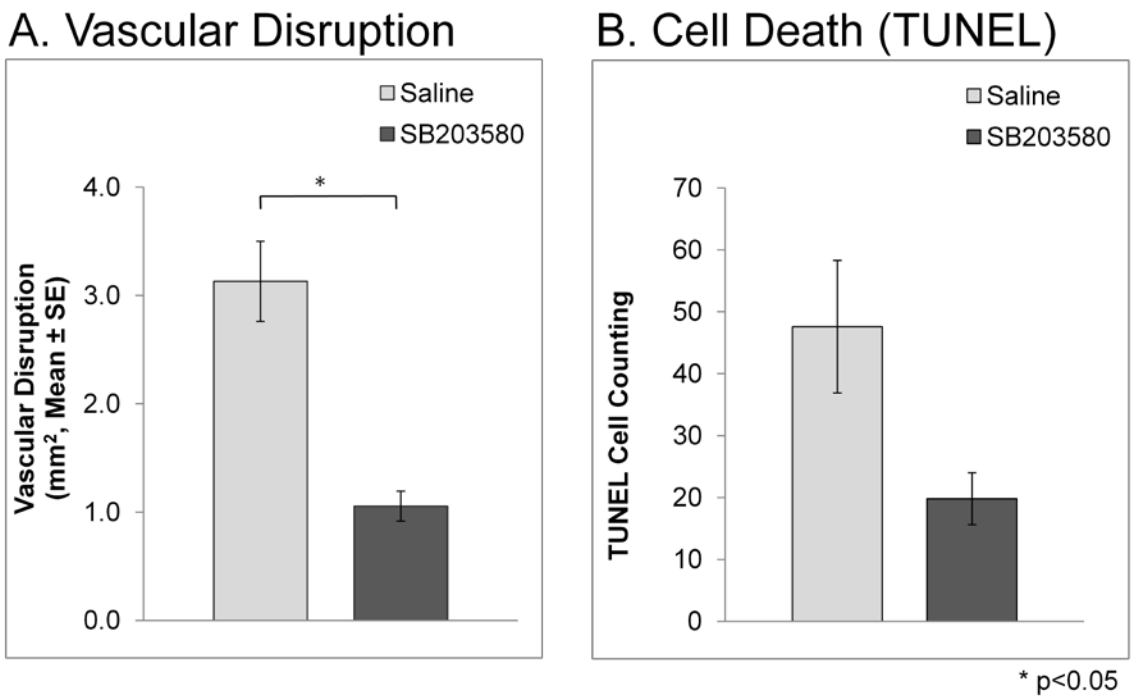

Figure 4. Inhibition of p38 kinase activity reduced ischemic injury

To verify if PAR1 mediated thrombin toxicity is dependent on MAPK kinases during ischemia, we infused SB203580 the antagonist to p38. (A) The area of FITC-dextran distribution was significantly less in the group treated with 10nmol inhibitor than in the vehicle group (Independent sample t-test, *P<0.05*). (B) The number of TUNEL positive cells in the agonist group also decreased than that in the control.

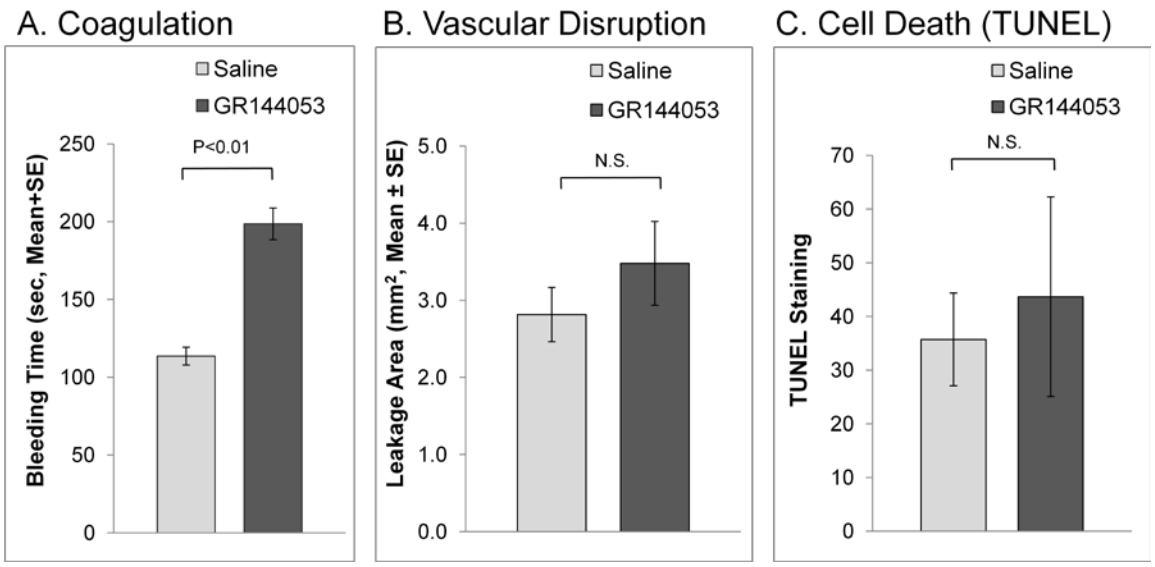

Figure 5. Inhibition of platelet aggregation did not affect ischemic vascular disruption

To examine if increased coagulation activity contributes to thrombin toxicity on the vasculature during ischemia, we infused GR144053 an inhibitor against platelet glycoprotein IIbIIIa during 4hr ischemia and reperfusion. (A) The overall coagulation activity was significantly increased in the treatment group compared to the vehicle group (Independent sample t-test, $P<0.05$). (B) No significant difference was found in the area of severe vascular disruption between the two groups ($P>0.05$). (C) The number of TUNEL positive cells in the treatment group was not significantly different from that in the control group ($P>0.05$).

V. CONCLUSION

This thesis investigated whether blood-brain barrier leakage contributes to ischemic injury by a thrombin-related mechanism. Although many efforts have been devoted to describe the molecular mechanisms underlying ischemic injury, it is still unclear why a certain group of cells die from a particular mechanism of death and why delayed neuronal death occurs after reperfusion. A comprehensive understanding on the microenvironment of brain cells and the dynamic interaction between different cells is needed to understand fully the heterogeneous nature of stroke pathophysiology. This thesis is part of the effort towards that goal.

The thesis established the notion that severe vascular disruption was associated with surrounding tissue injury. The application of high molecular weight marker FITC-dextran facilitated the labeling of original injury sites in the vasculature after we demonstrated a tight correlation between FITC-dextran extravasation and severe vascular injury. Features of cytotoxic edema were identified within these labeled vessels, and barrier dysfunction was exemplified by the discontinuous membrane ultrastructure. Histology staining for infarction and neuronal injury indicated that increased level of vascular leakage strongly correlated with increased tissue injury.

It then became an interesting question to know what mechanisms account for the link between vessel damage and tissue injury in acute ischemia. Vasogenic edema is a possible mechanism by allowing the water influx in the interstitial space and increasing the intracranial pressure, but in general

vasogenic edema does not become significant until hours or even days after the stroke onset. The fact that vascular disruption labeled by FITC-dextran appeared as early as 1hr after ischemia suggested the possibility of an early mediator leaking into the brain parenchyma and causing subsequent tissue injury.

The thesis presented evidence for the first time that blood-brain barrier leakage of thrombin contributed to severe brain injury in an *in vivo* ischemia model. Thrombin might exert its toxic effect by promoting microthrombosis within the vasculature, or by activating cellular receptors on the peri-vascular tissues, most likely via PAR1 receptor (Figure 5.1). Our data supported the model of cellular receptor pathways. Increased levels of thrombin and PAR1 activation were found in regions of severe vascular disruption. Arterial infusion of thrombin or PAR1 agonist exacerbated both severe vascular damage and tissue cell death, which was reduced by infusion of either thrombin inhibitor or PAR1 antagonist. One of the downstream effectors of PAR1, p38 MAP kinase, was tested and the result suggested that thrombin toxicity might involve the MAPK pathways.

The exact mechanism of how thrombin mediates vascular and tissue injury during acute ischemia requires further investigation. Thrombin toxicity on vasculature might be mediated by its direct effect on blood-brain barrier tight junctions, or by affecting neurons and glial cells which disrupts the integrity of neurovascular unit, or by inducing inflammatory response that brings indirect detrimental outcome to the brain. For future studies, cell-specific PAR1 knockout animals might be needed to dissect the roles of thrombin in different cell types.

Alternatively, virus-based shRNA could be infused to knock down the expression of PAR1 or other downstream genes. Novel markers that are able to detect thrombin activation *in vivo* are highly desired for research attempt to relate thrombin to pathophysiological changes during stroke.

Thrombin concentration in the systemic circulation is under delicate regulation. High level of thrombin contributes to the stroke risk by potential high incidence of microthrombosis, and low thrombin activity leads to intracerebral bleeding complications. The data from the thesis suggested a novel mechanism of thrombin toxicity that leaking thrombin in parenchymal tissue might play a significant role in causing brain injury during acute stage of ischemia. It provides the possibility of designing drugs that target only to the cellular receptor pathway without affecting coagulation activity. Argatroban, as well as many other inhibitors of thrombin, need to be re-evaluated for their efficacy in reducing thrombin toxicity in acute ischemia.

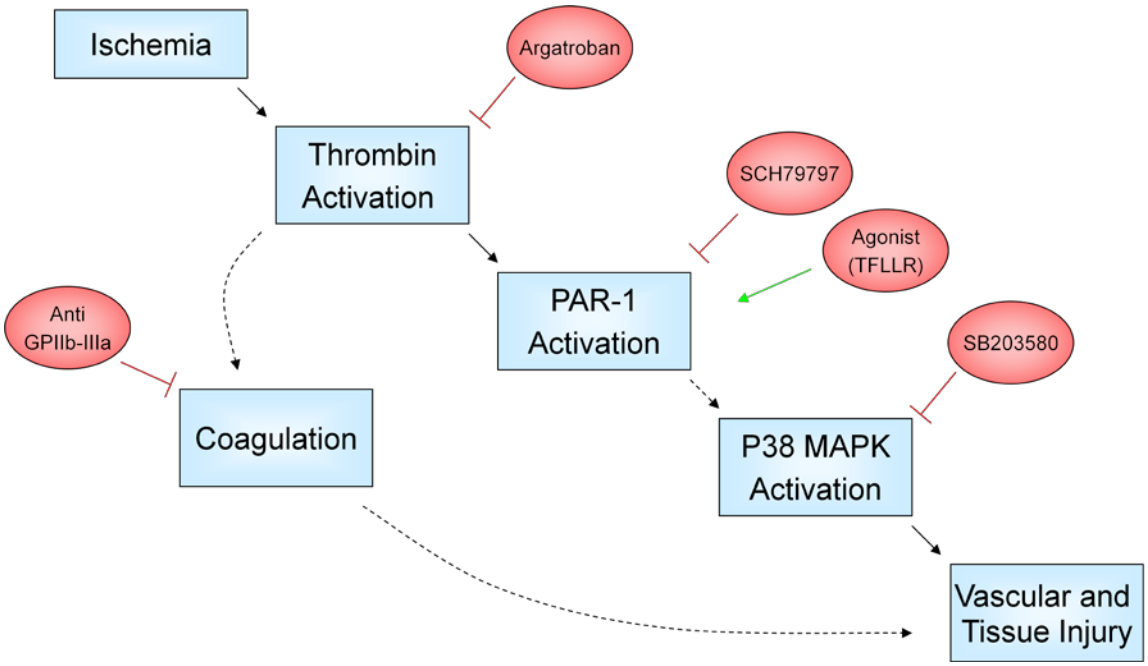

Figure 1. Scheme of thrombin toxicity during acute stage of ischemia

REFERENCE

1. Chen B, Friedman B, Cheng Q, Tsai P, Schim E, Kleinfeld D, Lyden PD. Severe blood-brain barrier disruption and surrounding tissue injury. *Stroke*. 2009;40:e666-674

2. Lo EH. A new penumbra: Transitioning from injury into repair after stroke. *Nat Med*. 2008;14:497-500

3. Ginsberg MD. Local metabolic responses to cerebral ischemia. *Cerebrovasc Brain Metab Rev*. 1990;2:58-93

4. Dirnagl U, Iadecola C, Moskowitz MA. Pathobiology of ischaemic stroke: An integrated view. *Trends Neurosci*. 1999;22:391-397

5. Tissue plasminogen activator for acute ischemic stroke. The national institute of neurological disorders and stroke rt-pa stroke study group. *N Engl J Med*. 1995;333:1581-1587

6. Reed SD, Cramer SC, Blough DK, Meyer K, Jarvik JG. Treatment with tissue plasminogen activator and inpatient mortality rates for patients with ischemic stroke treated in community hospitals. *Stroke*. 2001;32:1832-1840

7. Lo EH, Dalkara T, Moskowitz MA. Mechanisms, challenges and opportunities in stroke. *Nat Rev Neurosci*. 2003;4:399-415

8. Lo EH, Moskowitz MA, Jacobs TP. Exciting, radical, suicidal: How brain cells die after stroke. *Stroke*. 2005;36:189-192

9. Lipton P. Ischemic cell death in brain neurons. *Physiol Rev*. 1999;79:1431-1568

10. Martin RL, Lloyd HG, Cowan AI. The early events of oxygen and glucose deprivation: Setting the scene for neuronal death? *Trends Neurosci*. 1994;17:251-257

11. Fiskum G, Murphy AN, Beal MF. Mitochondria in neurodegeneration: Acute ischemia and chronic neurodegenerative diseases. *J Cereb Blood Flow Metab*. 1999;19:351-369

12. Chan PH. Reactive oxygen radicals in signaling and damage in the ischemic brain. *J Cereb Blood Flow Metab*. 2001;21:2-14

13. Murphy AN, Fiskum G, Beal MF. Mitochondria in neurodegeneration: Bioenergetic function in cell life and death. *J Cereb Blood Flow Metab*. 1999;19:231-245

14. Kroemer G, Reed JC. Mitochondrial control of cell death. *Nat Med*. 2000;6:513-519

15. Bernardi P, Petronilli V, Di Lisa F, Forte M. A mitochondrial perspective on cell death. *Trends Biochem Sci*. 2001;26:112-117

16. Yuan J, Yankner BA. Apoptosis in the nervous system. *Nature*. 2000;407:802-809

17. Nicotera P, Lipton SA. Excitotoxins in neuronal apoptosis and necrosis. *J Cereb Blood Flow Metab*. 1999;19:583-591

18. Budd SL, Tenneti L, Lishnak T, Lipton SA. Mitochondrial and extramitochondrial apoptotic signaling pathways in cerebrocortical neurons. *Proc Natl Acad Sci U S A*. 2000;97:6161-6166

19. Chopp M, Chan PH, Hsu CY, Cheung ME, Jacobs TP. DNA damage and repair in central nervous system injury: National institute of neurological disorders and stroke workshop summary. *Stroke*. 1996;27:363-369

20. Salvesen GS. A lysosomal protease enters the death scene. *J Clin Invest*. 2001;107:21-22

21. Yu SW, Wang H, Poitras MF, Coombs C, Bowers WJ, Federoff HJ, Poirier GG, Dawson TM, Dawson VL. Mediation of poly(adp-ribose) polymerase-1-dependent cell death by apoptosis-inducing factor. *Science*. 2002;297:259-263

22. Graham SH, Chen J. Programmed cell death in cerebral ischemia. *J Cereb Blood Flow Metab*. 2001;21:99-109

23. Wei L, Ying DJ, Cui L, Langsdorf J, Yu SP. Necrosis, apoptosis and hybrid death in the cortex and thalamus after barrel cortex ischemia in rats. *Brain Res*. 2004;1022:54-61

24. Garcia JH, Liu KF, Ho KL. Neuronal necrosis after middle cerebral artery occlusion in wistar rats progresses at different time intervals in the caudoputamen and the cortex. *Stroke*. 1995;26:636-642; discussion 643

25. Garcia JH, Liu KF, Ye ZR, Gutierrez JA. Incomplete infarct and delayed neuronal death after transient middle cerebral artery occlusion in rats. *Stroke*. 1997;28:2303-2309; discussion 2310

26. Garcia JH, Yoshida Y, Chen H, Li Y, Zhang ZG, Lian J, Chen S, Chopp M. Progression from ischemic injury to infarct following middle cerebral artery occlusion in the rat. *Am J Pathol*. 1993;142:623-635

27. Kirino T. Delayed neuronal death in the gerbil hippocampus following ischemia. *Brain Res*. 1982;239:57-69

28. del Zoppo GJ. Stroke and neurovascular protection. *N Engl J Med*. 2006;354:553-555

29. Rubin LL, Staddon JM. The cell biology of the blood-brain barrier. *Annu Rev Neurosci*. 1999;22:11-28

30. Sandoval KE, Witt KA. Blood-brain barrier tight junction permeability and ischemic stroke. *Neurobiol Dis*. 2008;32:200-219

31. Hawkins BT, Davis TP. The blood-brain barrier/neurovascular unit in health and disease. *Pharmacol Rev*. 2005;57:173-185

32. Nagaraja TN, Karki K, Ewing JR, Croxen RL, Knight RA. Identification of variations in blood-brain barrier opening after cerebral ischemia by dual contrast-enhanced magnetic resonance imaging and t 1sat measurements. *Stroke*. 2008;39:427-432

33. Nagaraja TN, Keenan KA, Fenstermacher JD, Knight RA. Acute leakage patterns of fluorescent plasma flow markers after transient focal cerebral ischemia suggest large openings in blood-brain barrier. *Microcirculation*. 2008;15:1-14

34. Belayev L, Busto R, Zhao W, Ginsberg MD. Quantitative evaluation of blood-brain barrier permeability following middle cerebral artery occlusion in rats. *Brain Res*. 1996;739:88-96

35. Albayrak S, Zhao Q, Siesjo BK, Smith ML. Effect of transient focal ischemia on blood-brain barrier permeability in the rat: Correlation to cell injury. *Acta Neuropathol*. 1997;94:158-163

36. Strbian D, Durukan A, Pitkonen M, Marinkovic I, Tatlisumak E, Pedrono E, Abo-Ramadan U, Tatlisumak T. The blood-brain barrier is continuously open for several weeks following transient focal cerebral ischemia. *Neuroscience*. 2008;153:175-181

37. Brown RC, Davis TP. Calcium modulation of adherens and tight junction function: A potential mechanism for blood-brain barrier disruption after stroke. *Stroke*. 2002;33:1706-1711

38. Cruzalegui FH, Bading H. Calcium-regulated protein kinase cascades and their transcription factor targets. *Cell Mol Life Sci*. 2000;57:402-410

39. Benarroch EE. Hypoxia-induced mediators and neurologic disease. *Neurology*. 2009;73:560-565

40. Kimura C, Oike M, Ito Y. Hypoxia-induced alterations in ca(2+) mobilization in brain microvascular endothelial cells. *Am J Physiol Heart Circ Physiol*. 2000;279:H2310-2318

41. Huber JD, Egleton RD, Davis TP. Molecular physiology and pathophysiology of tight junctions in the blood-brain barrier. *Trends Neurosci*. 2001;24:719-725

42. Jin KL, Mao XO, Greenberg DA. Vascular endothelial growth factor: Direct neuroprotective effect in in vitro ischemia. *Proc Natl Acad Sci U S A*. 2000;97:10242-10247

43. Greenberg DA, Jin K. From angiogenesis to neuropathology. *Nature*. 2005;438:954-959

44. Ohab JJ, Fleming S, Blesch A, Carmichael ST. A neurovascular niche for neurogenesis after stroke. *J Neurosci*. 2006;26:13007-13016

45. Zhang ZG, Zhang L, Jiang Q, Zhang R, Davies K, Powers C, Bruggen N, Chopp M. Vegf enhances angiogenesis and promotes blood-brain barrier leakage in the ischemic brain. *J Clin Invest*. 2000;106:829-838

46. Paul R, Zhang ZG, Eliceiri BP, Jiang Q, Boccia AD, Zhang RL, Chopp M, Cheresh DA. Src deficiency or blockade of src activity in mice provides cerebral protection following stroke. *Nat Med*. 2001;7:222-227

47. Weis S, Shintani S, Weber A, Kirchmair R, Wood M, Cravens A, McSharry H, Iwakura A, Yoon YS, Himes N, Burstein D, Doukas J, Soll R, Losordo D, Cheresh D. Src blockade stabilizes a flk/cadherin complex, reducing edema and tissue injury following myocardial infarction. *J Clin Invest*. 2004;113:885-894

48. Barone FC, Feuerstein GZ. Inflammatory mediators and stroke: New opportunities for novel therapeutics. *J Cereb Blood Flow Metab*. 1999;19:819-834

49. Stanimirovic D, Satoh K. Inflammatory mediators of cerebral endothelium: A role in ischemic brain inflammation. *Brain Pathol*. 2000;10:113-126

50. del Zoppo G, Ginis I, Hallenbeck JM, Iadecola C, Wang X, Feuerstein GZ. Inflammation and stroke: Putative role for cytokines, adhesion molecules and inos in brain response to ischemia. *Brain Pathol*. 2000;10:95-112

51. Frijns CJ, Kappelle LJ. Inflammatory cell adhesion molecules in ischemic cerebrovascular disease. *Stroke*. 2002;33:2115-2122

52. Allan SM, Rothwell NJ. Cytokines and acute neurodegeneration. *Nat Rev Neurosci*. 2001;2:734-744

53. Lo EH, Wang X, Cuzner ML. Extracellular proteolysis in brain injury and inflammation: Role for plasminogen activators and matrix metalloproteinases. *J Neurosci Res*. 2002;69:1-9

54. Yong VW, Power C, Forsyth P, Edwards DR. Metalloproteinases in biology and pathology of the nervous system. *Nat Rev Neurosci*. 2001;2:502-511

55. Wang X, Mori T, Jung JC, Fini ME, Lo EH. Secretion of matrix metalloproteinase-2 and -9 after mechanical trauma injury in rat cortical cultures and involvement of map kinase. *J Neurotrauma*. 2002;19:615-625

56. Gasche Y, Copin JC, Sugawara T, Fujimura M, Chan PH. Matrix metalloproteinase inhibition prevents oxidative stress-associated blood-brain barrier disruption after transient focal cerebral ischemia. *J Cereb Blood Flow Metab*. 2001;21:1393-1400

57. Gu Z, Kaul M, Yan B, Kridel SJ, Cui J, Strongin A, Smith JW, Liddington RC, Lipton SA. S-nitrosylation of matrix metalloproteinases: Signaling pathway to neuronal cell death. *Science*. 2002;297:1186-1190

58. Jian Liu K, Rosenberg GA. Matrix metalloproteinases and free radicals in cerebral ischemia. *Free Radic Biol Med*. 2005;39:71-80

59. Asahi M, Wang X, Mori T, Sumii T, Jung JC, Moskowitz MA, Fini ME, Lo EH. Effects of matrix metalloproteinase-9 gene knock-out on the proteolysis of blood-brain barrier and white matter components after cerebral ischemia. *J Neurosci*. 2001;21:7724-7732

60. Zhao BQ, Tejima E, Lo EH. Neurovascular proteases in brain injury, hemorrhage and remodeling after stroke. *Stroke*. 2007;38:748-752

61. Park KP, Rosell A, Foerch C, Xing C, Kim WJ, Lee S, Opdenakker G, Furie KL, Lo EH. Plasma and brain matrix metalloproteinase-9 after acute focal cerebral ischemia in rats. *Stroke*. 2009;40:2836-2842

62. Romanic AM, White RF, Arleth AJ, Ohlstein EH, Barone FC. Matrix metalloproteinase expression increases after cerebral focal ischemia in rats: Inhibition of matrix metalloproteinase-9 reduces infarct size. *Stroke*. 1998;29:1020-1030

63. Shimamura N, Matchett G, Solaroglu I, Tsubokawa T, Ohkuma H, Zhang J. Inhibition of integrin alphavbeta3 reduces blood-brain barrier breakdown in focal ischemia in rats. *J Neurosci Res*. 2006;84:1837-1847

64. Rosenberg GA, Estrada EY, Dencoff JE. Matrix metalloproteinases and timps are associated with blood-brain barrier opening after reperfusion in rat brain. *Stroke*. 1998;29:2189-2195

65. Lo EH. Experimental models, neurovascular mechanisms and translational issues in stroke research. *Br J Pharmacol*. 2008;153 Suppl 1:S396-405

66. Simard JM, Kent TA, Chen M, Tarasov KV, Gerzanich V. Brain oedema in focal ischaemia: Molecular pathophysiology and theoretical implications. *Lancet Neurol*. 2007;6:258-268

67. Xue M, Del Bigio MR. Acute tissue damage after injections of thrombin and plasmin into rat striatum. *Stroke*. 2001;32:2164-2169

68. Keep RF, Xiang J, Ennis SR, Andjelkovic A, Hua Y, Xi G, Hoff JT. Blood-brain barrier function in intracerebral hemorrhage. *Acta Neurochir Suppl*. 2008;105:73-77

69. Gingrich MB, Traynelis SF. Serine proteases and brain damage - is there a link? *Trends Neurosci*. 2000;23:399-407

70. Sheehan JJ, Tsirka SE. Fibrin-modifying serine proteases thrombin, tpa, and plasmin in ischemic stroke: A review. *Glia*. 2005;50:340-350

71. Pfefferkorn T, Staufer B, Liebetrau M, Bultemeier G, Vosko MR, Zimmermann C, Hamann GF. Plasminogen activation in focal cerebral ischemia and reperfusion. *J Cereb Blood Flow Metab*. 2000;20:337-342

72. Pfefferkorn T, Wiessner C, Allegrini PR, Staufer B, Vosko MR, Liebetrau M, Bueltemeier G, Kloss CU, Hamann GF. Plasminogen activation in experimental permanent focal cerebral ischemia. *Brain Res*. 2000;882:19-25

73. Wang YF, Tsirka SE, Strickland S, Stieg PE, Soriano SG, Lipton SA. Tissue plasminogen activator (tpa) increases neuronal damage after focal cerebral ischemia in wild-type and tpa-deficient mice. *Nat Med*. 1998;4:228-231

74. Yepes M, Sandkvist M, Moore EG, Bugge TH, Strickland DK, Lawrence DA. Tissue-type plasminogen activator induces opening of the blood-brain barrier via the ldl receptor-related protein. *J Clin Invest*. 2003;112:1533-1540

75. Liotta LA, Goldfarb RH, Brundage R, Siegal GP, Terranova V, Garbisa S. Effect of plasminogen activator (urokinase), plasmin, and thrombin on

glycoprotein and collagenous components of basement membrane. *Cancer Res*. 1981;41:4629-4636

76. Baramova EN, Bajou K, Remacle A, L'Hoir C, Krell HW, Weidle UH, Noel A, Foidart JM. Involvement of pa/plasmin system in the processing of pro-mmp-9 and in the second step of pro-mmp-2 activation. *FEBS Lett*. 1997;405:157-162

77. Adams RA, Passino M, Sachs BD, Nuriel T, Akassoglou K. Fibrin mechanisms and functions in nervous system pathology. *Mol Interv*. 2004;4:163-176

78. Coughlin SR. Thrombin signalling and protease-activated receptors. *Nature*. 2000;407:258-264

79. Davie EW, Fujikawa K, Kisiel W. The coagulation cascade: Initiation, maintenance, and regulation. *Biochemistry*. 1991;30:10363-10370

80. Jarvis GE, Atkinson BT, Frampton J, Watson SP. Thrombin-induced conversion of fibrinogen to fibrin results in rapid platelet trapping which is not dependent on platelet activation or gpib. *Br J Pharmacol*. 2003;138:574-583

81. Furie B, Furie BC. Thrombus formation in vivo. *J Clin Invest*. 2005;115:3355-3362

82. Lundblad RL, White GC, 2nd. The interaction of thrombin with blood platelets. *Platelets*. 2005;16:373-385

83. Hirano K. The roles of proteinase-activated receptors in the vascular physiology and pathophysiology. *Arterioscler Thromb Vasc Biol*. 2007;27:27-36

84. Wang H, Reiser G. Thrombin signaling in the brain: The role of protease-activated receptors. *Biol Chem*. 2003;384:193-202

85. Sokolova E, Reiser G. Prothrombin/thrombin and the thrombin receptors par-1 and par-4 in the brain: Localization, expression and participation in neurodegenerative diseases. *Thromb Haemost*. 2008;100:576-581

86. Junge CE, Sugawara T, Mannaioni G, Alagarsamy S, Conn PJ, Brat DJ, Chan PH, Traynelis SF. The contribution of protease-activated receptor 1 to neuronal damage caused by transient focal cerebral ischemia. *Proc Natl Acad Sci U S A*. 2003;100:13019-13024

87. Xi G, Reiser G, Keep RF. The role of thrombin and thrombin receptors in ischemic, hemorrhagic and traumatic brain injury: Deleterious or protective? *J Neurochem*. 2003;84:3-9

88. Luo W, Wang Y, Reiser G. Protease-activated receptors in the brain: Receptor expression, activation, and functions in neurodegeneration and neuroprotection. *Brain Res Rev*. 2007;56:331-345

89. Noorbakhsh F, Vergnolle N, Hollenberg MD, Power C. Proteinase-activated receptors in the nervous system. *Nat Rev Neurosci*. 2003;4:981-990

90. Fujimoto S, Katsuki H, Kume T, Akaike A. Thrombin-induced delayed injury involves multiple and distinct signaling pathways in the cerebral cortex and the striatum in organotypic slice cultures. *Neurobiol Dis*. 2006;22:130-142

91. Fujimoto S, Katsuki H, Ohnishi M, Takagi M, Kume T, Akaike A. Thrombin induces striatal neurotoxicity depending on mitogen-activated protein kinase pathways in vivo. *Neuroscience*. 2007;144:694-701

92. Fujimoto S, Katsuki H, Ohnishi M, Takagi M, Kume T, Akaike A. Plasminogen potentiates thrombin cytotoxicity and contributes to pathology of intracerebral hemorrhage in rats. *J Cereb Blood Flow Metab*. 2008;28:506-515

93. Ohnishi M, Katsuki H, Fujimoto S, Takagi M, Kume T, Akaike A. Involvement of thrombin and mitogen-activated protein kinase pathways in hemorrhagic brain injury. *Exp Neurol*. 2007;206:43-52

94. Lee KR, Betz AL, Keep RF, Chenevert TL, Kim S, Hoff JT. Intracerebral infusion of thrombin as a cause of brain edema. *J Neurosurg*. 1995;83:1045-1050

95. Lee KR, Betz AL, Kim S, Keep RF, Hoff JT. The role of the coagulation cascade in brain edema formation after intracerebral hemorrhage. *Acta Neurochir (Wien)*. 1996;138:396-400; discussion 400-391

96. Xi G, Keep RF, Hoff JT. Mechanisms of brain injury after intracerebral haemorrhage. *Lancet Neurol*. 2006;5:53-63

97. Kitaoka T, Hua Y, Xi G, Hoff JT, Keep RF. Delayed argatroban treatment reduces edema in a rat model of intracerebral hemorrhage. *Stroke*. 2002;33:3012-3018

98. Morris DC, Zhang L, Zhang ZG, Lu M, Berens KL, Brown PM, Chopp M. Extension of the therapeutic window for recombinant tissue plasminogen activator with argatroban in a rat model of embolic stroke. *Stroke*. 2001;32:2635-2640

99. Keep RF, Xi G, Hua Y, Hoff JT. The deleterious or beneficial effects of different agents in intracerebral hemorrhage: Think big, think small, or is hematoma size important? *Stroke*. 2005;36:1594-1596

100. Longa EZ, Weinstein PR, Carlson S, Cummins R. Reversible middle cerebral artery occlusion without craniectomy in rats. *Stroke*. 1989;20:84-91

101. Manoonkitiwongsa PS, Schultz RL, McCreery DB, Whitter EF, Lyden PD. Neuroprotection of ischemic brain by vascular endothelial growth factor is critically dependent on proper dosage and may be compromised by angiogenesis. *J Cereb Blood Flow Metab*. 2004;24:693-702

102. Bederson JB, Pitts LH, Tsuji M, Nishimura MC, Davis RL, Bartkowski H. Rat middle cerebral artery occlusion: Evaluation of the model and development of a neurologic examination. *Stroke*. 1986;17:472-476

103. Tsopanoglou NE, Maragoudakis ME. Inhibition of angiogenesis by small-molecule antagonists of protease-activated receptor-1. *Semin Thromb Hemost*. 2007;33:680-687

104. Yang S, Song S, Hua Y, Nakamura T, Keep RF, Xi G. Effects of thrombin on neurogenesis after intracerebral hemorrhage. *Stroke*. 2008;39:2079-2084

105. Striggow F, Riek M, Breder J, Henrich-Noack P, Reymann KG, Reiser G. The protease thrombin is an endogenous mediator of hippocampal neuroprotection against ischemia at low concentrations but causes degeneration at high concentrations. *Proc Natl Acad Sci U S A*. 2000;97:2264-2269

106. Maragoudakis ME, Tsopanoglou NE, Andriopoulou P. Mechanism of thrombin-induced angiogenesis. *Biochem Soc Trans*. 2002;30:173-177

107. Tsopanoglou NE, Maragoudakis ME. On the mechanism of thrombin-induced angiogenesis. Potentiation of vascular endothelial growth factor activity on endothelial cells by up-regulation of its receptors. *J Biol Chem*. 1999;274:23969-23976

108. Jiang Y, Wu J, Hua Y, Keep RF, Xiang J, Hoff JT, Xi G. Thrombin-receptor activation and thrombin-induced brain tolerance. *J Cereb Blood Flow Metab*. 2002;22:404-410

109. Xi G, Keep RF, Hua Y, Xiang J, Hoff JT. Attenuation of thrombin-induced brain edema by cerebral thrombin preconditioning. *Stroke*. 1999;30:1247-1255

110. Henrich-Noack P, Striggow F, Reiser G, Reymann KG. Preconditioning with thrombin can be protective or worsen damage after endothelin-1-induced focal ischemia in rats. *J Neurosci Res*. 2006;83:469-475

111. Furie B, Furie BC. Mechanisms of thrombus formation. *N Engl J Med*. 2008;359:938-949

112. Gavard J, Gutkind JS. Protein kinase c-related kinase and rock are required for thrombin-induced endothelial cell permeability downstream from galpha12/13 and galpha11/q. *J Biol Chem*. 2008;283:29888-29896

113. Komarova YA, Mehta D, Malik AB. Dual regulation of endothelial junctional permeability. *Sci STKE*. 2007;2007:re8

114. van Nieuw Amerongen GP, van Delft S, Vermeer MA, Collard JG, van Hinsbergh VW. Activation of rhoa by thrombin in endothelial hyperpermeability: Role of rho kinase and protein tyrosine kinases. *Circ Res*. 2000;87:335-340

115. Coughlin SR. Protease-activated receptors in hemostasis, thrombosis and vascular biology. *J Thromb Haemost*. 2005;3:1800-1814

116. Junge CE, Lee CJ, Hubbard KB, Zhang Z, Olson JJ, Hepler JR, Brat DJ, Traynelis SF. Protease-activated receptor-1 in human brain: Localization and functional expression in astrocytes. *Exp Neurol*. 2004;188:94-103

117. Traynelis SF, Trejo J. Protease-activated receptor signaling: New roles and regulatory mechanisms. *Curr Opin Hematol*. 2007;14:230-235

118. Kuliopulos A, Covic L, Seeley SK, Sheridan PJ, Helin J, Costello CE. Plasmin desensitization of the par1 thrombin receptor: Kinetics, sites of truncation, and implications for thrombolytic therapy. *Biochemistry*. 1999;38:4572-4585

119. Trivedi V, Boire A, Tchernychev B, Kaneider NC, Leger AJ, O'Callaghan K, Covic L, Kuliopulos A. Platelet matrix metalloprotease-1 mediates thrombogenesis by activating par1 at a cryptic ligand site. *Cell*. 2009;137:332-343

120. Ludeman MJ, Kataoka H, Srinivasan Y, Esmon NL, Esmon CT, Coughlin SR. Par1 cleavage and signaling in response to activated protein c and thrombin. *J Biol Chem*. 2005;280:13122-13128

121. Nesi A, Fragai M. Substrate specificities of matrix metalloproteinase 1 in par-1 exodomain proteolysis. *Chembiochem*. 2007;8:1367-1369

122. Nguyen M, Arkell J, Jackson CJ. Thrombin rapidly and efficiently activates gelatinase a in human microvascular endothelial cells via a mechanism

independent of active mt1 matrix metalloproteinase. *Lab Invest*. 1999;79:467-475

123. Borbiev T, Birukova A, Liu F, Nurmukhambetova S, Gerthoffer WT, Garcia JG, Verin AD. P38 map kinase-dependent regulation of endothelial cell permeability. *Am J Physiol Lung Cell Mol Physiol*. 2004;287:L911-918

124. Vandell AG, Larson N, Laxmikanthan G, Panos M, Blaber SI, Blaber M, Scarisbrick IA. Protease-activated receptor dependent and independent signaling by kallikreins 1 and 6 in cns neuron and astroglial cell lines. *J Neurochem*. 2008;107:855-870

125. Nozaki K, Nishimura M, Hashimoto N. Mitogen-activated protein kinases and cerebral ischemia. *Mol Neurobiol*. 2001;23:1-19

126. Strande JL, Hsu A, Su J, Fu X, Gross GJ, Baker JE. Sch 79797, a selective par1 antagonist, limits myocardial ischemia/reperfusion injury in rat hearts. *Basic Res Cardiol*. 2007;102:350-358

127. Matsuno H, Kozawa O, Ueshima S, Matsuo O, Collen D, Uematsu T. Lack of tpa significantly affects antithrombotic therapy by a gpiib/iiia antagonist, but not by a thrombin inhibitor in mice. *Thromb Haemost*. 2000;83:605-609

128. Matsuno H, Kozawa O, Okada K, Ueshima S, Matsuo O, Uematsu T. Inhibitors of fibrinolytic components play different roles in the formation and removal of arterial thrombus in mice. *J Cardiovasc Pharmacol*. 2002;39:278-286

129. Nishida M, Matsuno H, Kozawa O, Ueshima S, Matsuo O, Collen D, Uematsu T. Tpa, but not upa, significantly affects antithrombotic therapy by a glycoprotein iib/iiia antagonist, but not by a factor xa inhibitor. *J Cardiovasc Pharmacol*. 2000;36:770-775

130. de Garavilla L, Vergnolle N, Young SH, Ennes H, Steinhoff M, Ossovskaya VS, D'Andrea MR, Mayer EA, Wallace JL, Hollenberg MD, Andrade-Gordon P, Bunnett NW. Agonists of proteinase-activated receptor 1 induce plasma extravasation by a neurogenic mechanism. *Br J Pharmacol*. 2001;133:975-987

131. Kawao N, Hiramatsu K, Inoi N, Kuroda R, Nishikawa H, Sekiguchi F, Kawabata A. The par-1-activating peptide facilitates pepsinogen secretion in rats. *Peptides*. 2003;24:1449-1451

132. Cheng T, Liu D, Griffin JH, Fernandez JA, Castellino F, Rosen ED, Fukudome K, Zlokovic BV. Activated protein c blocks p53-mediated

apoptosis in ischemic human brain endothelium and is neuroprotective. *Nat Med*. 2003;9:338-342

133. Domotor E, Benzakour O, Griffin JH, Yule D, Fukudome K, Zlokovic BV. Activated protein c alters cytosolic calcium flux in human brain endothelium via binding to endothelial protein c receptor and activation of protease activated receptor-1. *Blood*. 2003;101:4797-4801

134. Hoxie JA, Ahuja M, Belmonte E, Pizarro S, Parton R, Brass LF. Internalization and recycling of activated thrombin receptors. *J Biol Chem*. 1993;268:13756-13763

135. Giacaman RA, Asrani AC, Ross KF, Herzberg MC. Cleavage of protease-activated receptors on an immortalized oral epithelial cell line by porphyromonas gingivalis gingipains. *Microbiology*. 2009;155:3238-3246

136. Vergnolle N, Wallace JL, Bunnett NW, Hollenberg MD. Protease-activated receptors in inflammation, neuronal signaling and pain. *Trends Pharmacol Sci*. 2001;22:146-152

137. Mannaioni G, Orr AG, Hamill CE, Yuan H, Pedone KH, McCoy KL, Berlinguer Palmini R, Junge CE, Lee CJ, Yepes M, Hepler JR, Traynelis SF. Plasmin potentiates synaptic n-methyl-d-aspartate receptor function in hippocampal neurons through activation of protease-activated receptor-1. *J Biol Chem*. 2008;283:20600-20611

138. Lee CJ, Mannaioni G, Yuan H, Woo DH, Gingrich MB, Traynelis SF. Astrocytic control of synaptic nmda receptors. *J Physiol*. 2007;581:1057-1081

139. Choi SH, Lee DY, Kim SU, Jin BK. Thrombin-induced oxidative stress contributes to the death of hippocampal neurons in vivo: Role of microglial nadph oxidase. *J Neurosci*. 2005;25:4082-4090

140. Chen D, Dorling A. Critical roles for thrombin in acute and chronic inflammation. *J Thromb Haemost*. 2009;7 Suppl 1:122-126